Interaction of Nitrogen/CO_2 Mixtures with Crude Oil

FINAL REPORT

Reporting period start date: June 1, 2005
Reporting period end date: December 31, 2006

By

Mario J. Farias and
Dr. Robert W. Watson

Report Issued: August 8, 2007

Penn State Sub-Contract No. : 2933-TPSU-DOE-2098
DOE Award Number: DE-FC26-04NT42098

The Pennsylvania State University
The College of Earth and Mineral Sciences
The Department of Energy and Geo-Environmental Engineering
The Energy Institute
University Park, PA 16802

DISCLAIMER

"This report was prepared as an account of work sponsored by an agency of the United States Government. Neither the United States Government nor any agency thereof, nor any of their employees, makes any warranty, express or implied, or assumed any legal liability or responsibility for the accuracy, completeness, or usefulness of any information, apparatus, product or process disclosed, or represents that its use would not infringe privately owned manufacturer, or otherwise does not necessarily constitute or imply its endorsement, recommendation, or favoring by the United States Government or any agency thereof. The views and opinions of authors expressed herein do not necessarily state or reflect those of the United States Government or any agency thereof."

ABSTRACT

The Oil & Gas Journal, in 2004, states that CO_2 flooding is the fastest-growing enhanced oil recovery technique in USA, and production derived from CO_2 projects has more than tripled from 50,000-Barrels/day to 200,000-Barrels/day. Cyclic injection of CO_2 and N_2 combines environmental benefits attendant to reducing CO_2 concentrations in the atmosphere and economic benefits realized through improving oil recovery. There are a number of variables involved in the design of a successful and profitable cyclic injection operation. The objective of this study is to investigate the influence of mechanisms such as gas solubility and oil vaporization on the cyclic injection process using laboratory experimentations. A PVT cell was used to perform six cycles of injection into a Chipmunk formation crude oil. Conditions of pressure and temperature in the cell are 150-psig and 70 ^{0}F. These conditions of pressure and temperature were maintained for five different injected mixtures of CO_2 and N_2. These mixtures were 100-%-0-%, 80-%-20-%, 53-%-47-%, 20-%-80-%, and 0-%-100-% of CO_2 and N_2 respectively. Laboratory results indicate a higher solubility of CO_2 when compared to that of N_2. Moreover, gas is more soluble during the first 3 to 4 cycles, and is independent of the composition of the injected mixture. Results also show that low hydrocarbon vaporization is realized using N_2. CO_2 by comparison shows a higher hydrocarbon vaporization effect than N_2 with maximum hydrocarbon extraction attained using CO_2 concentrations close to 100-% in the injected fluid. For pressure conditions at which experiments were performed, the results indicate that cyclic operations must consider the effect of gas solubility and hydrocarbons vaporization.

TABLE OF CONTENTS

Disclaimer ii
Abstract iii
Introduction 1
Executive summary 2
Literature review 4
    Cyclic injection process 4
Experimental and numerical study 9
    Previous experimental research on cyclic injection 10
    Experimental setup and methodology 13
    The equation of state 16
    Properties prediction 20
Results and discussion 21
    Experimental results 21
    Numerical results 30
Conclusions 38
    Future research 38
References 40
Nomenclature 42

LIST OF GRAPHICAL MATERIAL

Figure 1: Schematic of one cycle in the cyclic injection process 5
Figure 2: Carbon Dioxide pressure-temperature diagram (Chemical logic Co., 1999)... 6
Figure 3: Nitrogen phase diagram (Wray, E.M, 1972) 7
Figure 4: Original composition phase diagram of Big Andy crude oil (Sample 1)..... 9
Figure 5: Original composition phase diagram of Chipmunk crude oil (Sample 2)..... 10
Figure 6: Sample 1 phase diagram of oil after 6 injection cycles using different gas mixtures 13
Figure 7: PVT cell schematic diagram..... 13
Figure 8: PVT cell experimental setup..... 15
Figure 9: PVT cell differential pressures versus number of cycles 22
Figure 10: Experiment 1 gas composition, non-hydrocarbon components and total hydrocarbons versus number of cycles..... 23
Figure 11: Experiment 2 gas composition, non-hydrocarbon components and total hydrocarbons versus number of cycles..... 23
Figure 12: Experiment 3 gas composition, non-hydrocarbon components and total hydrocarbons versus number of cycles..... 24
Figure 13: Experiment 4 gas composition, non-hydrocarbon components and total hydrocarbons versus number of cycles..... 24
Figure 14: Experiment 5 gas composition, non-hydrocarbon components and total hydrocarbons versus number of cycles..... 25
Figure 15: Experiment 1 gas composition versus cycle, hydrocarbon components..... 26
Figure 16: Experiment 2 gas composition versus cycle, hydrocarbon components..... 26
Figure 17: Experiment 3 gas composition versus cycle, hydrocarbon components..... 27
Figure 18: Experiment 4 gas composition versus cycle, hydrocarbon components..... 27
Figure 19: Experiment 5 gas composition versus cycle, hydrocarbon components..... 28
Figure 20: Sample 2 crude oil P-T diagram for experiments 1, 2 and 3 after 6 cycles.. 29
Figure 21: Sample 2 crude oil P-T diagram for experiments 3, 4 and 5 after 6 cycles.. 29
Figure 22: Schematic of experimental cyclic injection..... 31
Figure 23: Gas composition from experiment 4 versus cycle, (non-hydrocarbons)..... 31
Figure 24: Gas composition from experiment 3 versus cycle, (non-hydrocarbons)..... 32

Figure 25: Gas composition from experiment 2 versus cycle, (non-hydrocarbons)..... 32
Figure 26: Gas composition from experiment 1 versus cycle, (non-hydrocarbons)..... 33
Figure 27: Oil composition from experiment 4 versus cycle, (non-hydrocarbons) 33
Figure 28: Oil composition from experiment 3 versus cycle, (non-hydrocarbons) 34
Figure 29: Oil composition from experiment 2 versus cycle, (non-hydrocarbons)..... 34
Figure 30: Oil composition from experiment 1 versus cycle, (non-hydrocarbons)..... 35
Figure 31: Oil composition from experiment 4 versus cycle, (C_7, C_8, C_9, C_{10+})..... 35
Figure 32: Oil composition from experiment 3 versus cycle, (C_7, C_8, C_9, C_{10+})..... 36
Figure 33: Oil composition from experiment 2 versus cycle, (C_7, C_8, C_9, C_{10+})..... 36
Figure 34: Oil composition from experiment 1 versus cycle, (C_7, C_8, C_9, C_{10+})..... 37

LIST OF TABLES

Table 1: Sample 1 oil composition after 6 injection cycles..... 12
Table 2: Injection gas compositions used in experiments..... 14
Table 3: Sample 2, gas and oil composition after 6 cycles of injection..... 23

INTRODUCTION

The implementation of enhanced oil recovery techniques (EOR) is often necessary to maintain operations in reservoirs realizing depletion and declining production rates. In general, field operators consider two major factors during the design of enhanced recovery operations: technique practicability and economic viability. The feasibility of the process is related to reservoir and reservoir fluid characteristics and the economics that are associated with the cost of the technique and the success of its implementation. EOR techniques can be classified into three major categories: thermal, chemical, and gas injection (immiscible or miscible). This study will focus on gas injection and the recovery mechanisms related to it. Various gases are used for gas injection operations; hydrocarbons, air, flue gases, Carbon Dioxide, Nitrogen, and sometimes mixtures of two or more of the aforementioned gases. This investigation focuses on gas injection operations that use Carbon Dioxide (CO_2) and Nitrogen (N_2) mixtures.

Another objective of this investigation is to develop an understanding of mechanisms attendant to cyclic gas injection. Recently, gas cyclic injection has been the focus of attention among petroleum producing corporations. This is due to the small upfront investment and the relatively quick pay out. The technique of cyclic injection has been studied for years and oil viscosity reduction, gas swelling, reservoir properties, injected fluid, number of cycles, and quantity of injected fluid have been identified as the most important parameters impacting performance of CO_2 and N_2 cyclic operations. Given the added benefit that the use of CO_2 for cyclic injection in oil reservoirs can reduce its concentration in the atmosphere, the process is also considered to be environmentally friendly. A series of experiments were conducted using mixtures of CO_2 and N_2 to investigate this technique.

EXECUTIVE SUMMARY

A Nitrogen Huff and Puff process has been utilized to stimulate oil production in the Big Andy field located in eastern Kentucky. This Nitrogen stimulation project has been ongoing for over 6 years and has resulted in a four fold increase in oil production. Nitrogen is generated on site by processing atmospheric air utilizing membrane separation technology. The membrane separation technology yields Nitrogen at a cost of approximately $1.00 per MCF that contains volumetrically up to 5-percent Oxygen. Analysis of the field's production performance indicates that it requires the injection of approximately 2.5 MCF of Nitrogen to recover one barrel of oil. Also, given the fact that a significant increase in oil production has been realized, the question becomes what is the long term effect of Nitrogen injection on the crude oil remaining in the reservoir.

The objective of a Stripper Well Consortium Project has been to develop an understanding of the phase behavior of N_2/O_2 gases in the presence of hydrocarbons. In order to meet this objective, a PVT system was fabricated so that the impact on the physical properties of the crude oil of Nitrogen injection could be measured. System validation tests were completed with propane, methane/propane and propane/ethane mixtures at different temperatures. Pressure-versus-specific volume data were generated and verified by comparison to values in the literature. A phase behavior computer package was developed and tuned using data obtained from both the field and laboratory.

Field experience has indicated that periodic injection of CO_2 mixed with Nitrogen has improved the volumetric flow rate of the wells. It is postulated that the CO_2 tends to remove skin damage in the near well bore area. Also, it is understood that CO_2 is miscible in oil. The objective of this project is to evaluate the behavior of N_2/CO_2 injection and its impact on the recovery process. Moreover, it is likely that future legislation will mandate a reduction in CO_2 levels that are generated through hydrocarbon combustion. A means of sequestering this CO_2 is to inject it into oil and gas horizons. It is likely that the injection of CO_2 can result in improved recovery from these horizons. The crude oil evaluated is obtained from the Big Andy Field in Kentucky and the Chipmunk sandstone in Cattaraugus County, New York. It is anticipated that the results of these studies will be used as the underpinnings to subsequent field tests.

The approach adopted in this study is to confirm the previous findings of other investigations using laboratory and numerical studies. The purpose of the experimental study is to develop an understanding of the reaction between hydrocarbons and injected CO_2-N_2 mixtures, and the structure of the resulting phase diagram. The object of the numerical study is to reproduce the experimental data and permit an in-depth analysis of the parameters that are crucial to cyclic injection.

Through laboratory experiments, a zero-dimensional model (PVT cell) was used to mimic the cyclic injection process and to develop an understanding of the behavior of crude oil when CO_2-N_2 gas mixture is injected into it. Upon completion of the experiments, we had realized a better understanding of the compositional changes occurring during the recovery process. Furthermore, a phase equilibrium model was

developed to represent the thermodynamics of the cyclic injection process. The phase equilibrium package was used to replicate data generated during the experimental stage.

It was concluded that the extrapolation of laboratory results to the field setting is not direct, but reasonable qualitative conclusions about the process can be drawn. Laboratory results indicate that CO_2 vaporizes more components in larger quantities than N_2. This is shown in Table 3. Laboratory results also indicate that N_2 is more soluble in the oil than CO_2. The results indicate that 0.34-% mole-percent of N_2 as compared to 0.17-% mole-percent of CO_2 dissolve in the oil. Finally, laboratory results also indicate that more oil is vaporized using CO_2 than that vaporized using N_2.

The tuned EOS package predicted the changes in composition with the number of injection-soaking-withdrawal cycles. The tuning of EOS parameters, such as attraction parameter, the co-volume parameter, and the binary interaction coefficients, was accomplished through the matching of experimental data. The final EOS parameters were in the range of 5-% to 20-% of the values found in pertinent literature.

LITERATURE REVIEW

Primary production employs the reservoir's natural energy or reservoir initial pressure for oil recovery purposes. When the reservoir's own energy is not sufficient to maintain oil production, methods to increase production rate and ultimate recovery need to be applied. These methods are referred to as enhanced oil recovery (EOR) techniques. The concepts associated with EOR techniques are well known, the field application of waterflooding and gas injection dates back to the 1800's. Experimental studies and field pilot tests of techniques such as thermal recovery and Carbon Dioxide injection date back to the 1950's. The increase in oil and gas demand worldwide has motivated a renewed interest in EOR research among the scientific and industrial community. Consequently, new research to understand the mechanisms involved in EOR methods is currently needed.

EOR techniques are classified into three major categories: thermal injection, chemical injection, and gas injection. This work is focused on gas injection, which is the EOR technique that is pertinent to this study. In terms of oil recovered attendant to its application, this technique is second only to steam flooding (Jarrell, 2002). Reservoir pressure maintenance and the stabilization of production levels were the primary purposes for early adoption of gas injection. Another justification for gas injection was to maintain pressure to avoid condensation in retrograde reservoirs. A variety of gases can be used for the improved recovery of oil, with each having advantages and disadvantages depending on reservoir and operation conditions. Typical gases used during gas injection operations are Carbon Dioxide, Nitrogen, hydrocarbon, flue gas and air.

One of the latest EOR surveys provides evidence that indicates that Carbon Dioxide flooding is the fastest-growing EOR technique in USA (Oil & Gas Journal, 2004). Since 1980, production resulting from EOR processes such as thermal and chemical injection has fallen sharply. Meanwhile, production derived from Carbon Dioxide projects has more than tripled.

Every gas injection process is designed to improve oil recovery, but each differs in the way that the injection takes place. Typically, gas injection refers to a gas flooding process. Conceptually, gas injection and cyclic gas injection are considerably different. In a flooding process, a slug of gas is injected from multiple wells into the reservoir. The gas propagates through the formation to one or multiple producing wells. In cyclic injection practices, gas is injected into a single well. This same well is then shut-in for a period of time, and then following this shut-in period, returned to production. In the next section, more details of the cyclic injection process are presented.

Cyclic injection process

The principle of cyclic injection, also known as Huff'n Puff process, lies in the application of the treatment to a single well treatment. Gas injection occurs in batches into a single well, shutting it in after every injection. The shut-in period, defined as

soaking time, permits gas migration into the reservoir and time for an interaction between the injected gas and the crude-oil to occur. In theory, by the end of the shut-in period, the region around wellbore contains low viscosity oil, free gas, and immobile water (Patton et al., 1982). Production resumes after the shut-in period. A cycle, by definition, begins with gas injection and ends when the production rate has dropped to below an economic limit (Figure 1). Cyclic gas injection is usually an immiscible process, meaning that injection takes places below the thermodynamic minimum miscibility pressure (MMP). The focal point of this investigation rests in the predominant mechanisms that govern cyclic injection below MMP.

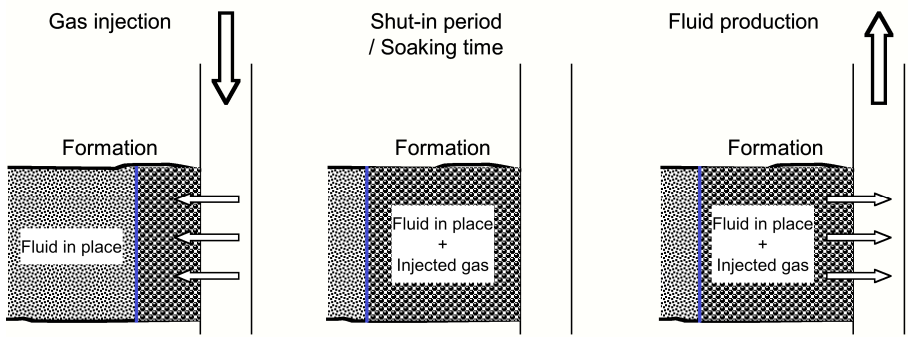

Figure 1: Schematic of one cycle in the cyclic injection process

Gas availability, corrosive effect, and environmental impact, are some of the factors taken into consideration when evaluating Carbon Dioxide and Nitrogen as injecting fluids. Carbon dioxide (CO_2) is a stable, nontoxic compound found in a gaseous state at standard conditions. It has been applied successfully in gas flooding projects for heavy oils. CO_2 is a very versatile gas, but when dissolved in water its corrosive effect has a negative impact on equipment. Furthermore, CO_2 in the presence of water forms carbonic acid, which can negatively affect injectivity in carbonate reservoirs. Carbon Dioxide is soluble in reservoir oils, causing viscosity reduction and oils swelling. The phase behavior of CO_2 (Figure 2) is of importance for use in the design of injection operations. Knowing its phase-state for various operating conditions (pressure and temperature) gives a better understanding of its behavior at reservoir conditions.

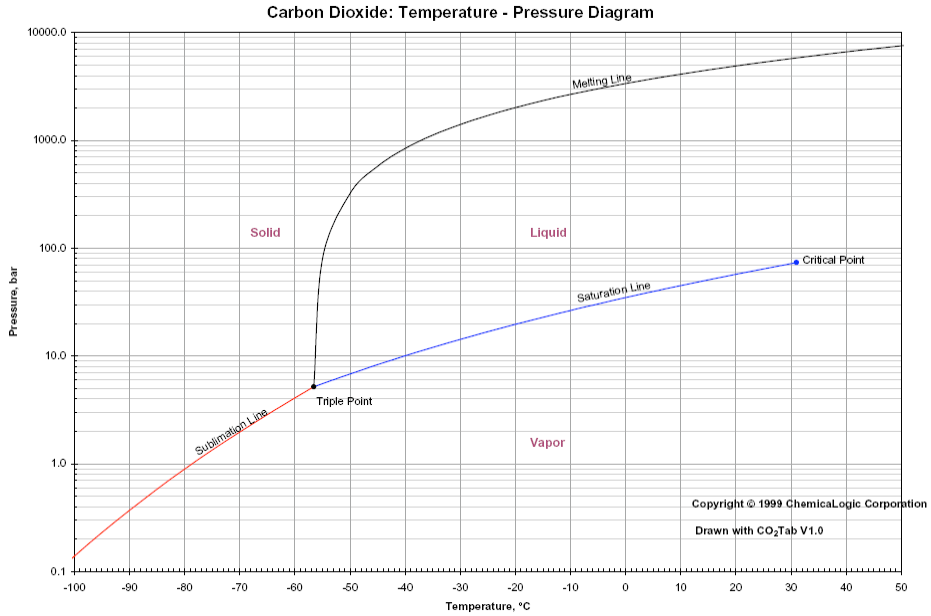

Figure 2: Carbon Dioxide pressure-temperature diagram (Chemical logic Co., 1999)

Some of the important justifications for the use of N_2 include gas availability, good injectivity in low permeability reservoirs, negligible environmental impact, existence in a gaseous state at standard conditions (see Figure 3), and superior recoveries when compared to alternative EOR methods (Whitson, 2000). Since N_2 is an inert gas, it does not contribute to corrosion of equipment. The behavior of N_2 is similar to that of CO_2, in the sense that, both are not first contact miscible. When Nitrogen is used as injection fluid, it dissolves into the oil and trades place with lighter ends of crude oil. This exchange positively influences oil mobility with a resulting improvement in oil recovery. N_2 has a lower solubility in oil and less of an impact on oil properties than CO_2.

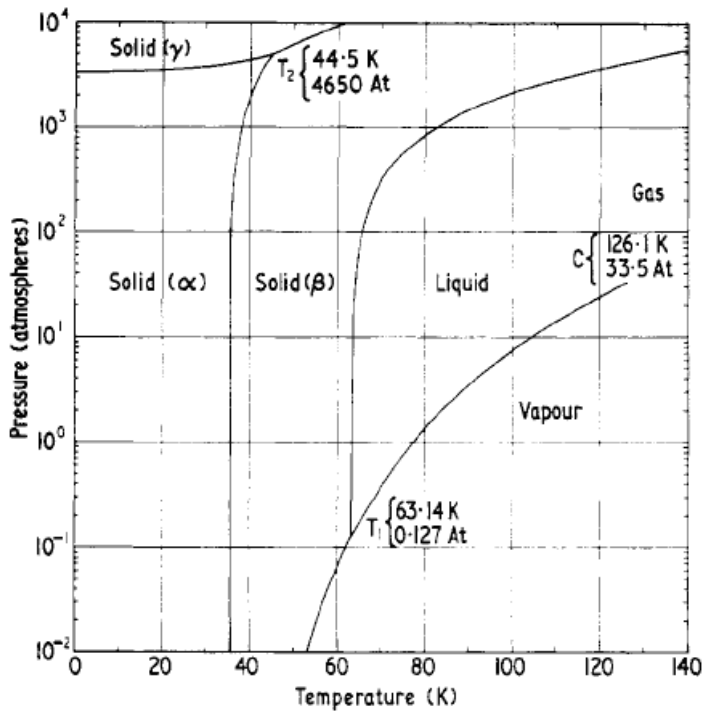

Figure 3: Nitrogen phase diagram (Wray, E.M, 1972)

There are three major mechanisms to consider during gas cyclic injection: oil swelling, oil viscosity reduction and water blockage. The oil swells because gas dissolves into the oil, creating oil saturation augmentation; hence increasing oil's relative permeability and its mobility. Gas dissolved into the crude oil reduces its viscosity. In the case of heavy crude oils, this reduction amounts to the extent of one order of magnitude (Denoyelle and Lemonniere, 1987). In the case of light crude oils, the reduction is up to five times (Simpson, 1988). Water saturation tends to decrease since the oil and gas saturations are increasing with gas injection. Further, the increase in oil and gas saturation near the wellbore tends to displace the water back into the reservoir and away from the wellbore.

The technique of cyclic injection is not a recent discovery; early studies using CO_2 identified the most important parameters associated with the performance of these operations. Oil recovery showed a high sensitivity to factors such as volume of injected CO_2 per cycle, number of cycles and backpressure during production. In compilations of previous published project reports (Jarrell, 2002; Patton et al., 1982), cyclic CO_2 injection is recognized as an economically viable oil recovery technique.

In the late 1980's, field and experimental studies suggested that the driving mechanisms of CO_2 and N_2 injection include, but are not limited to, oil swelling, relative permeability and hydrocarbon vaporization during cyclic injection. It was also reported that a stock tank barrel of incremental oil is produced per every 2-MSCF of injected CO_2 and larger injection volumes result in greater increments. Further investigation on the effect of reservoir pressure was recommended (Haskin and Alston, 1989; Monger and Coma, 1988). Furthermore, in a summary report of EOR projects up to 1987, 20 fields

were active and more than 115 wells were realizing cyclic injection. On average, these fields used between 1.3 to 2-MSCF of CO_2 per incremental stock tank barrel of produced oil (Brock and Bryant, 1989).

In 1990, Thomas et al. investigated the impact during cyclic operations of gravitational segregation and remaining oil on oil recovery. It was confirmed that gravity segregation facilitates CO_2 penetration into the reservoir resulting in improved oil recovery. Additionally, these experimental and numerical studies showed an increase in oil recovery when a higher remaining oil saturation is present. In a five-year update report, Miller et al. reported that the implementation of CO_2 treatment on 240-wells resulted in 1-bbl of incremental oil above primary recovery for every 1.6-MSCF of CO_2 used. The Huff and Puff process was shown to be economically feasible for shallow light oil reservoirs (Miller and Bardon, 1994).

More recently, Mohammed-Sing (2006) suggested that CO_2 improves oil recovery due to oil viscosity reduction, oil swelling and near wellbore damage removal. In their sixteen project review, they highlighted as favorable factors in cyclic operations the following: high oil saturations, formation thicknesses, soaking intervals of 2 to 4-weeks, high injection volumes and rates, and a maximum of 3 cycles. They proposed optimizing the Huff and Puff process according to operating pressure, permeability and viscosity. A recent study demonstrated applicability of cyclic injection into a gas condensate reservoir (Al-Wadhahi et al., 2007). Using a validated numerical model, they confirmed that condensate revaporization is an influential mechanism for this type of reservoirs. The liquid revaporization occurred during the injection and soaking stages of the cyclic process, hence, improving gas production when production is resumed. It was noted in this study that wellbore skin resulting from liquid dropout was also mitigated.

EXPERMENTAL AND NUMERICAL STUDIES

The assessment of the interaction between injected gas and oil, notwithstanding the recovery method employed, requires that reservoir conditions be mimicked as closely as possible during laboratory tests. Attention also must to be paid to the composition of injection gas during the determination of its effect upon reservoir fluids.

The current investigation used oil samples from two different field projects: the Big Andy field located in Kentucky and the Chipmunk field that straddles the border between New York and Pennsylvania. The Big Andy field is an extension of a bigger field, the Big Sinking field, which is located in Eastern Kentucky. Drilling operations in this field started in the 1930's and currently it has over 400 active wells (Abboud, 2005). In the Big Andy reservoir, formation thickness is 40-*ft* and the depth to the top of the formation is about 1300-*ft*. Reservoir's porosity is approximately 16-% and its absolute permeability is approximately 19-*md*. This formation is considered to be highly fractured. During the mid 1980's, waterflooding operations were initiated but due to the presence of the natural fractures, it was unsuccessful. As a consequence, CO_2 injection and N_2 injection were implemented as an alternative enhanced recovery technique, the latter being currently in use. Big Andy crude is considered to be light crude oil given its API gravity of 68.9º. Even though this crude is considered to be light, its major components are heavier ends (C_7, C_8, C_9 and C_{10+}) that amount to 62.8-% by molar percent. The crude has a molecular weight of 104.4-$\frac{lb}{lbmol}$ and a density of 44.03 -$\frac{lb}{ft^3}$. For this work, the definition of Big Andy crude and Sample 1 will be used interchangeably. Figure 4 shows the phase diagram, critical pressure, critical temperature, and overall composition of Sample 1.

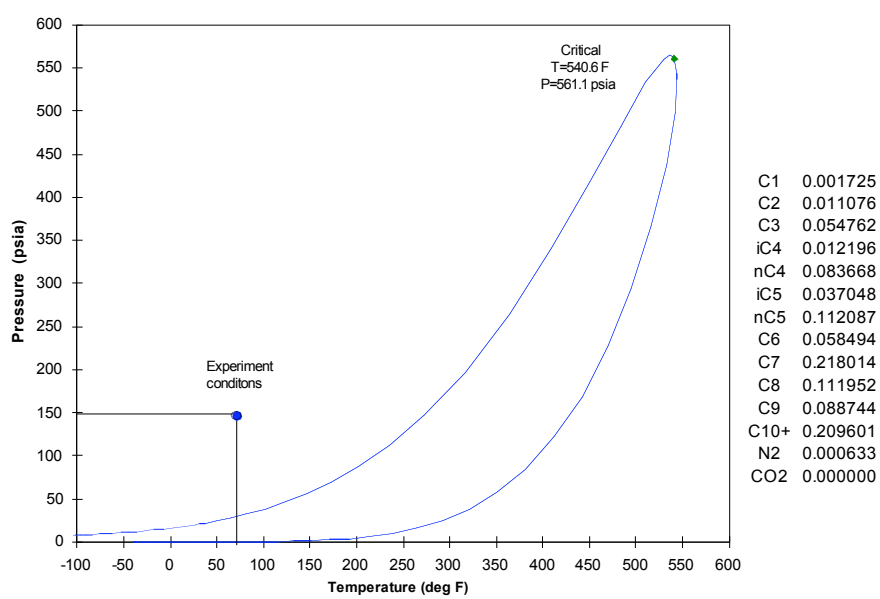

Figure 4: Original composition phase diagram of Big Andy crude oil (Sample 1)

The Chipmunk field is part of the larger Bradford field. The Bradford field is located in northern Pennsylvania and extends across the state line into New York State. Records of first oil production from this field go back to the late 1800's (Stanonis, 1958). The Chipmunk formation is a 40-*ft* thick sandstone and the depth to top of the formation is approximately 800-*ft*. The reservoir's porosity is about 20-% with permeability values ranging from 33-*md* down to 0.5-*md*. This formation is considered to be a tight sand. For more than 50 years, operators have implemented waterflooding with mixed results (Benson, 1998). As with Sample 1, the crude oil is light with API gravity of 60.3º API. Heavier ends (C_7, C_8, C_9 and C_{10+}) constitute around 80-% of the overall composition. Fluid properties such as molecular weight and liquid density are 128.9-$\frac{lb}{lbmol}$ and 46.02-$\frac{lb}{ft^3}$, respectively. Figure 5 contains a plot of the phase diagram. On Figure 5 are plotted the critical pressure and critical temperature for the crude oil used in the experiments. Also shown on Figure 5 is the overall composition of the oil. From this point forward, the definition of Chipmunk crude oil or Sample 2 will be used interchangeably. Both figures (Figure 4 and Figure 5) contain a plot of experiment conditions of temperature and pressure and its position with respect to the phase diagram.

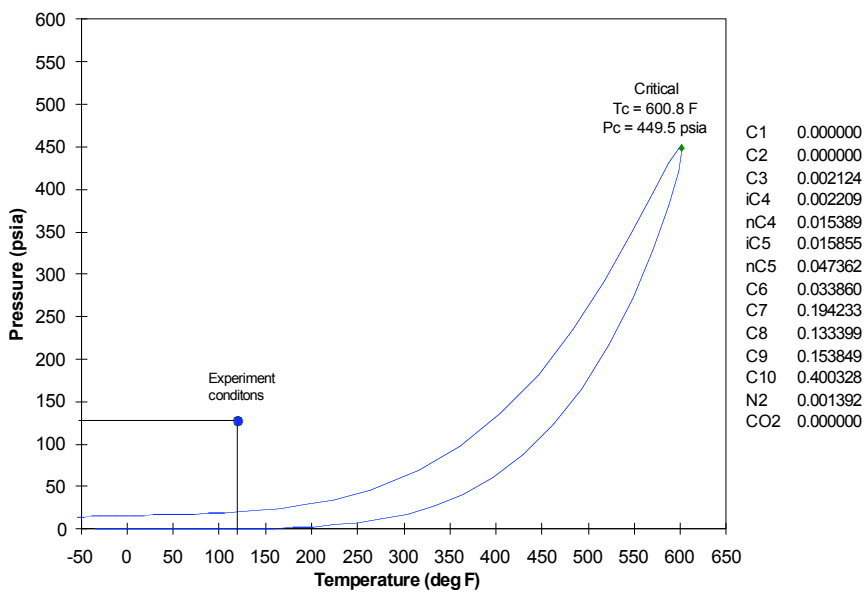

Figure 5: Original composition phase diagram of Chipmunk crude oil (Sample 2)

Previous experimental research on cyclic injection

Among the previous experimental investigations on cyclic gas injection, two are considered to be of particular importance to this research. The two projects are: "Evaluation of alternative gases for immiscible cyclic injection" (Shayegi, 1997) and "A

study of cyclic injection of Nitrogen on mid-continent crude oil: an investigation of the vaporization process in low pressured shallow reservoirs" (Abboud, 2005). The significance of these projects to current work is their experimental approach, discussed later in this section. Furthermore, they are among the latest experimental works performed on cyclic injection and the current investigation is an extension of Abboud's work.

Shayegi's investigation describes the effects of using Carbon Dioxide, methane, Nitrogen, and mixture of these gases on the cyclic injection process. Her experiments were conducted at immiscible conditions using sandstone cores containing residual oil following waterflooding. Her observations did not speak to the effect of absolute permeability or relative permeability. This is of note given that the cores used had different values of permeability. Shayegi noted that because of the efficiency of CO_2 when compared to the efficiency realized using other gases; CO_2 was the gas of choice in cyclic processes. Using pure CO_2, the recovery of the residual oil was greater than that attained with the other two gases. Additionally, mixtures of CO_2–N_2 and CO_2–CH_4 showed the highest oil recovery. As indicated by Shayegi:

> "Pure methane recovered approximately the same amount of waterflood residual oil as CO_2, whereas pure Nitrogen recovered about half that amount. Certain CO_2/N_2 and CO_2/CH_4 combinations yielded outstanding results, recovering 2-3 times the waterflood residual oil produced by CO_2 alone. Maximum recovery was obtained with combinations containing 10-25% CO_2."

Despite the fact that Shayegi did not indicate it, the cyclic injection process was proven, once again, to be a reliable and effective process for use in enhanced oil recovery. This assertion is made because any of the produced oil is part of the residual oil from a previous waterflood. This observation supports this initiative to expand research in the area of gas cyclic injection.

A question suggested by Shayegi's investigation is, how successful could this process be if the number of cycles is increased? During the current research, this idea is investigated by increasing the number of injection cycles to six for every experiment and through the development of a reservoir simulator where the number of injection cycles can be limitless.

Abboud's investigation on gas cyclic injection focused on the effect of Nitrogen and Nitrogen-Oxygen mixtures on oil composition. Specifically, the effect of the cyclic injection process on oil vaporization and the oil shrinkage factor was considered. Moreover, he developed a phase equilibrium package capable of modeling results from the experiments. There exists a close relationship between Abboud's investigation and this work. First, the experimental conditions of both investigation, such as volume, pressure and temperature, are the same. Secondly, this investigation uses outputs from Abboud's experiments as well as the same crude oil (Sample 1). Finally, the

methodology is the same for both investigations. This includes the number of injection-soaking-production cycles, duration of the soaking time and quantity of gas injected.

Findings in Abboud's investigation indicate an increase in oil viscosity and density at the end of six injection cycles that resulted from vaporization of hydrocarbons. It was noted that light hydrocarbons (C_1-C_4) had more of a tendency to vaporize than medium (C_5-C_9) and heavy (C_{10+}) hydrocarbon components. Table 1 shows the final composition of oil phase upon completion of each experiment. These results are consistent with the fact that lighter component have less cohesive force than heavier components. Because of this stripping effect, initial weight of oil showed a decrease in mass of up to 8.5-%.

Table 1: Sample 1 oil composition after 6 injection cycles

	Pre-injection	Post-injection		
	Original	100%N_2-0%O_2	97%N_2-3%O_2	86%N_2-14%O_2
C1	0.001725	0.000432	0.000000	0.000000
C2	0.011076	0.000000	0.000587	0.000000
C3	0.054762	0.013981	0.018697	0.014614
iC4	0.012196	0.006413	0.006586	0.005962
nC4	0.083668	0.057218	0.057737	0.053922
iC5	0.037048	0.030418	0.031307	0.029454
nC5	0.112087	0.102842	0.102108	0.098760
C6	0.058494	0.059487	0.056683	0.057745
C7	0.218014	0.236467	0.226008	0.231993
C8	0.111952	0.122888	0.116532	0.120190
C9	0.088744	0.100812	0.099459	0.100413
C10+	0.209601	0.268190	0.281283	0.285368
N2	0.000633	0.000852	0.003013	0.001579
CO2	0.000000	0.000000	0.000000	0.000000

Abboud's investigation was the first to consider compositional changes during the gas cyclic injection process. No previous experimental investigation had studied changes in the composition of fluids resulting from this enhanced recovery technique. Abboud also indicated that the impact in the final oil composition from the usage of different gas mixtures is small; this is after six cycles of injection. Figure 6 shows the slight difference in the final crude oil phase diagram following the six-cycles of injection, soaking and production.

For the different mixtures of gas injected, the phase diagrams of crude oil after each of the experiments have a tendency to be shifted to the right of the original composition. This tendency is evidence of the stripping effect of injected gas, confirming the vaporization of light ends (C_1-C_4), and eventually increasing the molar fraction of heavy components (C_5-C_{10+}). Appendix A contains plots of oil phase and gas phase composition per cycle; these plots are based on the results of the experimental tests completed using Sample 1.

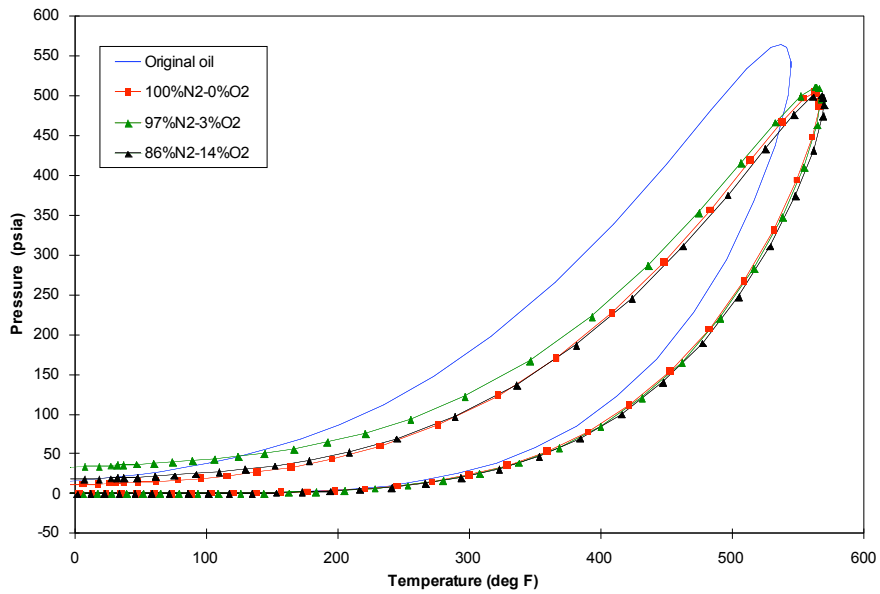

Figure 6: Sample 1 phase diagram of oil after 6 injection cycles using different gas mixtures

Experimental setup and methodology

The previous studies that were discussed in Section 4.1 set the starting point for the design of the experiments. In this work as in Abboud's work, a PVT cell was used to perform the six cycles of injection-soaking-production. The PVT cell's setup (Figure 7) consists of:

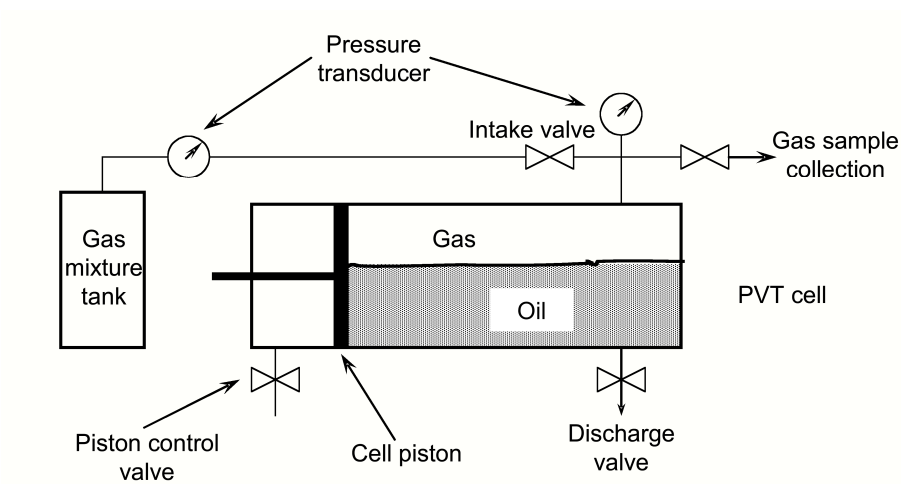

Figure 7: PVT cell schematic diagram

- A stainless steel cylinder with a maximum volume capacity of 500-*cc*, and a maximum operational pressure and temperature of 5000-*psig* and 350-^{o}F, respectively,
- a hydraulic pump for piston displacement purposes,
- two pressure transducers,
- a mixture tank containing injection gas,
- an intake valve to control volume of injected fluid,
- an exhaust valve for gas sample collection,
- a discharge valve for liquid sample collection.

The experimental conditions of pressure and temperature are 150-*psig* and 70-^{o}F respectively. These conditions were chosen to mimic reservoir conditions of pressure and temperature. The cell volume was set to 400-*cc*, held constant for all cycles of injection-soaking-production, and 250-*cc* of Sample 2 oil was placed in the cell.

A cycle, by definition, begins at the time of gas injection and ends when the cell is re-opened and the free gas is purged from the cell. In this investigation and that of Assad's, the number of cycles considered is six. Based on Assad's observations, we anticipate that a number of cycles larger that six will have minimal impact on the recovery process. The 24-hour period was determined to be the duration of the soaking period that would permit the achievement of thermodynamic equilibrium. By definition thermodynamic equilibrium is achieved when mass transfer between the liquid and the vapor phase attains equilibrium. Based on field practices and Shayegi's and Abboud's investigations, the gases selected for the experiments are Carbon Dioxide and Nitrogen. The mixtures between CO_2 and N_2 consider a range from 100-% CO_2 and 0-% N_2 to 0-% CO_2 and 100-% N_2 (Table 2).

Table 2: Injection gas compositions used in experiments

	SAMPLE 2
Experiment No. 1	100%CO_2-0%N_2
Experiment No. 2	88%CO_2-12%N_2
Experiment No. 3	53%CO_2-47%N_2
Experiment No. 4	20%CO_2-80%N_2
Experiment No. 5	0%CO_2-100%N_2

Other than the quality of injected gas, the pressure, the temperature and the volume were held constant for all tests. The experimental procedure is detailed as follows and every experiment was performed following these same steps. The photograph on Figure 8 shows the experimental setup used to determine the PVT properties of the oil.

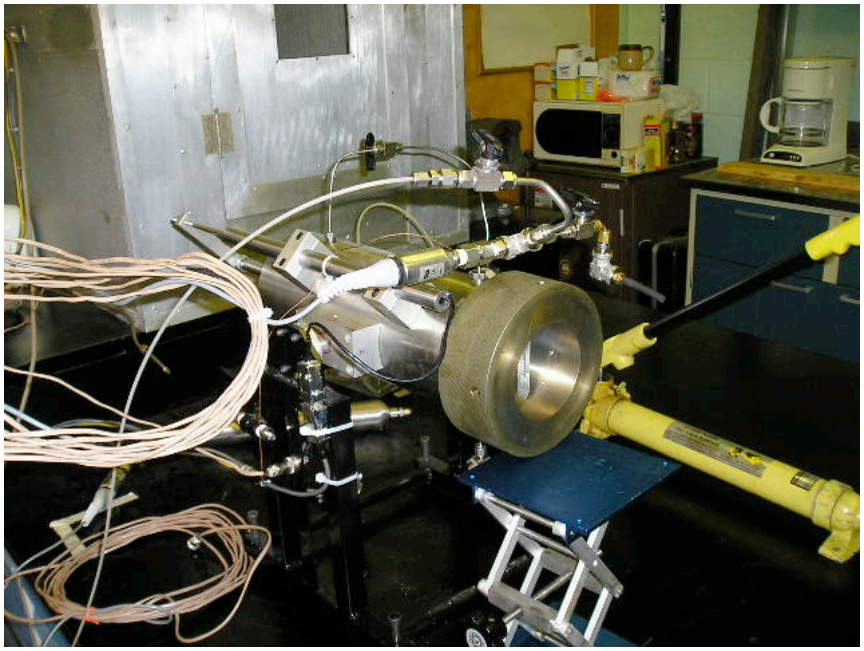

Figure 8: PVT cell experimental setup

1. Initial volume of crude is placed in the PVT cell. The action of piston motion displaces any gas from the cell through the collection valve. By doing this, only liquid remains in the cell.
2. Gas from the mixture tank is injected into the sealed cell; resulting in the cell regaining desired conditions of volume (400-*cc*) and pressure (150-*psig*).
3. At this point in the experiment, the soaking period begins and lasts for 24-hours. The cell configuration allows for full mixing of fluids because the apparatus can be rocked and the soaking period of 24-hours permits the attainment of thermodynamic equilibrium.
4. Sample of the gas is obtained through the opening of the collection valve. Excess gas is then vented. The cell is then purged of any remaining gas by moving the piston.
5. The next cycle is begun by injecting the next batch of gas, and the cell is returned to a volume of 400-*cc* and a pressure of 150-*psig*.
6. This procedure is repeated for six cycles.

7. A gas chromatographic analysis is performed on every gas sample obtained to determine its composition. Likewise, at the completion of the sixth cycle, a compositional analysis of the remaining crude oil in the cell is made.

The equation of state

This section contains the development of the phase behavior model (PBM) used to predict the volumetric and phase equilibrium of mixtures. The PBM uses the Peng-Robinson equation of state (EOS), which is an analytical expression relating pressure, temperature and volume (Peng and Robinson, 1976). Furthermore, EOS solution is used to calculate pressure-dependant fluid properties ensuring consistency in a thermodynamic model. This PBM model was created using class notes on phase behavior of petroleum fluids (Ayala H, Spring, 2005). The importance of a developed PBM lies in its usage. First, it is used as an independent tool for phase composition determination with experimental data. Second, it is used as one of the constitutive equation needed in a reservoir simulator.

The usage of an EOS in compositional reservoir simulation calls for two basic parameters, the phase compressibility factor (z) and component fugacity (fi). These parameters are a function of pressure, temperature and phase composition. Consequently, an equation of state sets forth the relationships governing pressure, temperature and phase composition.

There have been many EOS's used to calculate physical properties and vapor-liquid equilibrium of hydrocarbon mixtures. The flash calculations in current compositional model use the Peng-Robinson EOS (Eq.1). The PR-EOS is widely used in reservoir fluid studies because of its relative simplicity and accuracy. One of its principal advantages is its capability to accurately predict liquid phase density (Ahmed, 1989). The PR-EOS is a two-constant cubic equation of state derived from the real gas law.

$$p = \frac{RT}{v_m} - \frac{(a\alpha)_m}{v_m(v_m + b_m) + b_m(v_m - b_m)} \qquad \text{(Eq.1)}$$

where:

p = system pressure, psia
R = universal gas constant, 10.73 psia ft^3 / lb_{moles}ºR
T = system temperature, ºR
v_m = molar volume, ft^3 / lb_{mole}
$(a\alpha)_m$ = mixture attraction parameter, psia $(ft^3)^2$ / lb_{mole}^2
b_m = mixture co-volume parameter, ft^3 / lb_{mole}

A number of empirical based EOS's have been developed to predict compressibility factors for hydrocarbon mixtures as well as for both liquid and vapor phases. Coats

(1985) formulated a generalized equation that represents all cubic equations of state. Coats' general equation is a cubic expression for compressibility factor (z) (Eq.2)

$$z^3 + \left[\left(m_1 + m_2 - 1\right)B - 1\right]z^2 + \left[A + m_1 m_2 B^2 - \left(m_1 + m_2\right)B\left(B+1\right)\right]z - \left[AB + m_1 m_2 B^2\left(B+1\right)\right] = 0 \qquad \text{(Eq.2)}$$

where:

$$A = \sum_i^{n_c}\sum_j^{n_c} c_i c_j \left(a\alpha\right)_m \qquad \text{(Eq.3)}$$

$$\left(a\alpha\right)_m = \left(1 - \delta_{ij}\right)\left(\left(a\alpha\right)_i \left(a\alpha\right)_j\right)^{0.5} \qquad \text{(Eq.4)}$$

$$\left(a\alpha\right)_i = \Omega_{ai}\left[1 + m_i(1 - T_{ri}^{0.5})\right]^2 \frac{p_{ri}}{T_{ri}^2} \qquad \text{(Eq.5)}$$

$$B = b_m = \sum_{i=1}^{n_c} c_i b_i \qquad \text{(Eq.6)}$$

$$b_i = \Omega_{bi}\frac{p_{ri}}{T_{ri}} \qquad \text{(Eq.7)}$$

$$m_1 = 1 + \sqrt{2} \qquad \text{(Eq.8)}$$

$$m_2 = 1 - \sqrt{2} \qquad \text{(Eq.9)}$$

$$m_i = \begin{cases} 0.374640 + 1.54226\omega_i - 0.26992\omega_i^2 & \text{if } \omega_i \le 0.49 \\ 0.379642 + 1.48503\omega_i - 0.164423\omega_i^2 - 0.01666\omega_i^3 & \text{if } \omega_i \ge 0.49 \end{cases} \qquad \text{(Eq.10}$$

c_i, c_j = mole fraction of component in the phase

$\left(a\alpha\right)_i$ = component attraction parameter

b_i = component co-volume parameter

Ω_{ai} = component attraction parameter constant, 0.457235 used if no individual information is available

Ω_{bi} = component co-volume parameter constant 0.077796 used if no individual information is available

$p_{ri} = \dfrac{p}{p_{ci}}$ = component reduced pressure

$T_{ri} = \dfrac{T}{T_{ci}}$ = component reduced temperature

ω_i = component Pitzer's accentric factor

Thermodynamic equilibrium is achieved when all net transfer (heat, momentum, mass) is zero. Therefore, the fugacity of each component of the phases present must be the same. The thermodynamic phase equilibrium expression is written as:

$$f_{li} = f_{gi} \qquad \text{(Eq.11)}$$

where:

f_{li} = fugacity of component 'i' in the liquid phase

f_{gi} = fugacity of component 'i' in the gas phase

The concept of fugacity provides another constraint for the equilibrium between phases, and it is referred to as the capacity of a component to escape from one phase to the other. The fugacity coefficient is the ratio of the fugacity of a material to its partial pressure and can be calculated using the Peng-Robinson equation of state according to Eq.12:

$$\ln\phi_i = -\ln(Z-B) + \frac{A}{(m_1-m_2)B}\left(\frac{2\sum_{i=1}^{n_c}(a\alpha)_m c_i}{A} - \frac{b_i}{B}\right)\ln\left[\frac{Z+m_2B}{Z+m_1B}\right] + \frac{b_i}{B}(Z-1) \qquad \text{(Eq.12)}$$

where:

$\phi_i = \dfrac{f_i}{c_i p}$ fugacity coefficient of component 'i'

The Rachford-Rice objective function is an expression of the phase equilibrium in terms of weight of each component and its molar fraction. This function is the basis of flash calculations. It defines the amount and composition of the vapor phase and liquid phase, given the pressure, temperature and overall composition. The objective function (Eq.13) and its derivative (Eq.14) are stated as follows:

$$g(f_{ng}) = \sum_{i=1}^{n_c}\frac{c_i(K_i-1)}{1+f_{ng}(K_i-1)} = 0 \qquad \text{(Eq.13)}$$

$$g'(f_{ng}) = \sum_{i=1}^{n_c}\frac{c_i(K_i-1)}{\left[1+f_{ng}(K_i-1)\right]^2} \qquad \text{(Eq.14)}$$

where:

f_{ng} = vapor fraction in the mixture,

c_i = mole fraction of component i in the phase,

K_i = equilibrium constant ratio for component i, =(yi/xi),

This material balance equation is iteratively solved for the vapor phase fraction 'f_{ng}' using the Newton-Rapshon method:

$$f_{ng}^{new} = f_{ng}^{old} - \frac{g(f_{ng}^{old})}{g'(f_{ng}^{old})} \qquad \text{(Eq.15)}$$

The equilibrium constant or equilibrium ratio represents the equilibrium of phases and is expressed in Eq.16. The successive substitution method (SSM) is the iterative solution for the determination of equilibrium constants. The SSM technique is used to achieve the convergence to K_i, the thermodynamic equilibrium. The improvement in the 'K_i' value per iteration is shown in Eq.17.

$$K_i = \frac{\phi_{li}}{\phi_{gi}} = \frac{f_{li}/(x_i P)}{f_{gi}/(y_i P)} = \frac{y_i}{x_i}\left(\frac{f_{li}}{f_{gi}}\right) \qquad \text{(Eq.16)}$$

$$K_i^{n+1} = K_i^{n}\left\{\frac{f_{li}}{f_{gi}}\right\}^{n} \qquad \text{(Eq.17)}$$

where:

x_i = molar fraction of component 'i' in the liquid phase
y_i = molar fraction of component 'i' in the vapor phase

Properties prediction

The molecular weight for each phase is calculated by using the molar fractions of the corresponding phase, namely vapor (Eq.18) or liquid (Eq.19).

$$Mw_g = \sum_{i=1}^{n_c} y_i Mw_i \qquad \text{(Eq.18)}$$

$$Mw_l = \sum_{i=1}^{n} x_i Mw_i \qquad \text{(Eq.19)}$$

The density of a phase 'f' is calculated using its compressibility factor (z_a) as predicted by the Peng Robinson equation of state. From the real gas law, the density is expressed as:

$$\rho_f = \frac{P}{RT}\left(\frac{Mw_f}{Z_f}\right) \qquad \text{(Eq.20)}$$

To compute the viscosities of the phases, Lee-Gonzalez-Eakin correlation (Eq.21) was used to estimate the gas phase viscosity and Lohrenz, Bray & Clark correlation (Eq.25) was used to estimate the liquid viscosity.

$$\mu_g = 1 \cdot 10^{-4} k_v EXP\left(x_v \left(\frac{\rho_g}{62.4} \right)^{y_v} \right) \quad \text{(Eq.21)}$$

where:

$$k_v = \frac{\left(9.4 + 0.02MW_g\right)T^{1.5}}{209 + 19MW_g + T} \quad \text{(Eq.22)}$$

$$y_v = 2.4 - 0.2x_v \quad \text{(Eq.23)}$$

$$x_v = 3.5 + \frac{986}{T} + 0.01MW_g \quad \text{(Eq.24)}$$

$$\mu_l = \mu^* + \xi_m^{-1}\left[\left(0.1023 + 0.023364\rho_r + 0.058533\rho_r^2 - 0.040758\rho_r^3 + 0.0093724\rho_r^4\right)^4 - 1 \cdot 10^{-4}\right] \quad \text{(Eq.25)}$$

where:

$$\mu^* = \frac{\sum_i x_i \mu_i^* \sqrt{MW_i}}{\sum_i x_i \sqrt{MW_i}} \quad \text{(Eq.26)}$$

$$\mu_i^* = \frac{17.78 \cdot 10^{-5}\left(4.58T_{ri} - 1.67\right)^{0.625}}{\xi_i} \quad \text{(Eq.27)}$$

$$\xi_i = \frac{5.4402T_{ci}^{1/6}}{\sqrt{MW_i}P_{ci}^{2/3}} \quad \text{(Eq.28)}$$

RESULTS AND DISCUSSION

As previously noted, the results of the investigations of Shayegi and Abboud in cyclic gas injection were used as the starting point for this laboratory investigation. In this section, the results obtained from the five tests performed using different quality-mixtures of the gases are discussed. Injected mixtures differ from one another in terms of the amount of Carbon Dioxide and Nitrogen used.

Experimental results

An objective of this work is to investigate the interaction between the injected gases and the crude oil. For this reason, attention is paid to the pressure changes inside the PVT cell. Changes in pressure are indicative of the relative solubility of the gas in oil. Figure 9 shows the pressure variation per cycle between the initial injection pressure (150-*psig*) and the pressure measured at equilibrium conditions. A pressure transducer was used to continuously monitor the pressure inside the vessel. The difference in measured pressure qualitatively represents the amount of gas going into solution using the different injected gas mixtures.

As indicated in figure 9, the larger the content of CO_2 in the injected gas, the higher the pressure-drop during the soaking period. The largest pressure-drop (98-*psig*) measured during the first cycle was obtained using 100-% CO_2-0-% N_2. For subsequent experiments, as the percentage of CO_2 in the injected gas decreased, smaller pressure-drops were measured. Further, the trends of the differential pressure versus cycle number indicate that as the amount of CO_2 in the injection gas decreases, the smaller the change in differential pressure. Additionally, the change in differential pressure is more pronounced for experiments with higher concentrations of CO_2. As an example, experiments 1 and 2 show a gradient in differential pressure of about 30-*psi* between cycle 1 and cycle 2. In contrast, the same experiments exhibit a change in the differential pressure of 1-*psi* for the last two cycles. On the other hand, the variation in the differential-pressure for experiments 4 and 5 is approximately 9-*psi* between the first two cycles. And for the last two cycles, the differential pressure gradient is 1-*psi*.

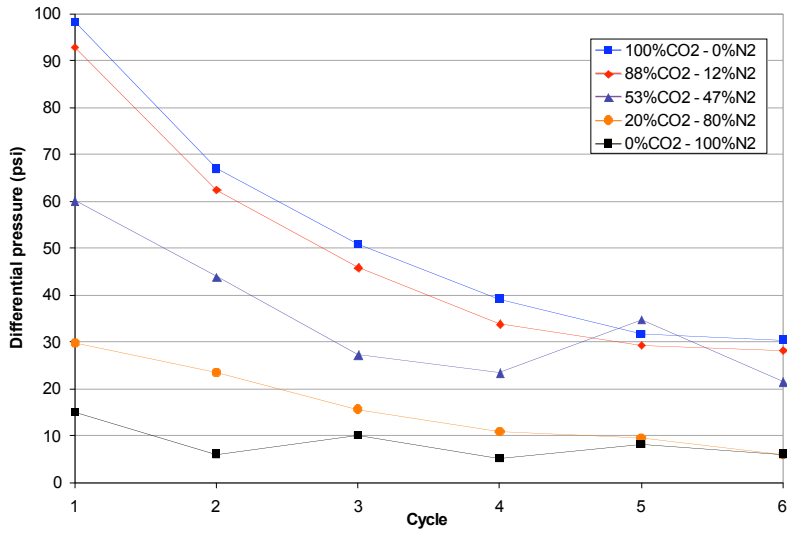

Figure 9: PVT cell differential pressures versus number of cycles

These observations are evidence of the gas solubility. As indicated by Jarrell (2002) and Stalkup (1983), this behavior is indicative of the higher solubility of CO_2 when compared to that of N_2. Moreover, both CO_2 and N_2 gases are more soluble during the first 3 to 4 cycles given that the oil has yet to be contacted by gas. As the number of cycles increases, the solubility of the gas in the oil decreases. Our tests also indicate that the gas solubility is dependent on the composition of the injected gas. For this investigation, the results indicate that the higher the CO_2 content in the injected gas, the higher the pressure-drop inside the PVT cell.

The gas recovered from the PVT cell is representative of the vapor phase at equilibrium conditions. Changes in gas composition result from the vaporization of the crude oil into the injected CO_2 and/or N_2. The gas composition is determined using chromatographic analysis after every cycle. For future reference in this work, the definition of gas and vapor are used interchangeably and non-hydrocarbon components refer to CO_2 and N_2. Summary of results are shown in a tabular form on Table 3. Figures 10 to 14 illustrate overall composition of the recovered gas, specifying the percentage of non-hydrocarbon components (CO_2 and N_2) and the summation of hydrocarbon components. Similarly, Figures 15 to 19 show the hydrocarbon components (C_3 to C_{7+}) present in the gas.

Table 3: Sample 2, gas and oil composition after 6 cycles of injection

	Original oil	100%CO_2		88%CO_2-12%N_2		53%CO_2-47%N_2		20%CO_2-80%N_2		0%CO_2-100%N_2	
	Comp.	GAS	OIL	GAS	OIL	GAS	OIL	GAS	OIL	GAS	OIL
C3	0.00212	0.005469	0.00075	0.00064	0.00000	0.00066	0.000000	0.000636	0.000000	0.000807	0.000000
iC4	0.00221	0.000072	0.00106	0.00002	0.00049	0.00002	0.000000	0.000021	0.000875	0.000029	0.001251
nC4	0.01539	0.006929	0.01026	0.00155	0.00562	0.00146	0.000000	0.001310	0.008106	0.001754	0.011449
iC5	0.01586	0.000102	0.01219	0.00006	0.01207	0.00005	0.002926	0.000043	0.008839	0.000062	0.012299
nC5	0.04736	0.004253	0.04390	0.00227	0.02772	0.00184	0.001073	0.001762	0.032453	0.002490	0.042975
C6	0.03386	0.001887	0.03479	0.00148	0.02557	0.00112	0.002859	0.001304	0.026847	0.002033	0.032255
C7+	0.88181	0.002774	0.89363	0.00320	0.92342	0.00261	0.991615	0.002644	0.918928	0.004150	0.896351
N2	0.00139	0.083643	0.00170	0.16550	0.00192	0.57911	0.001527	0.797110	0.002494	0.988676	0.003420
CO2	0.00000	0.894216	0.00173	0.82528	0.00319	0.41313	0.000000	0.195169	0.001458	0.000000	0.000000

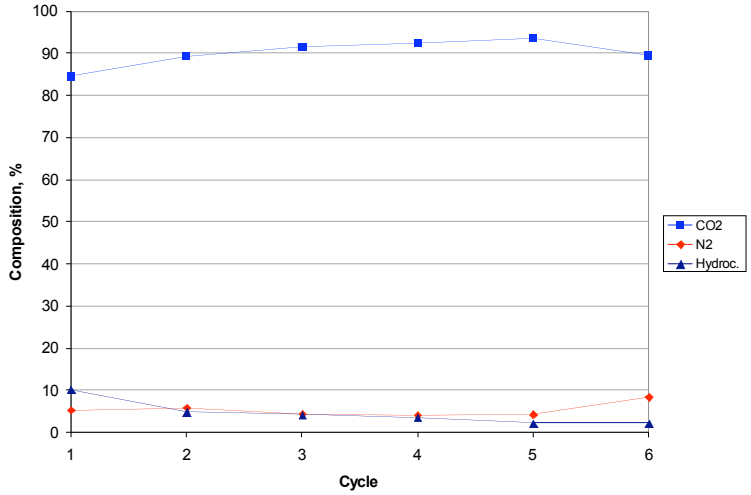

Figure 10: Experiment 1 gas composition, non-hydrocarbon components and total hydrocarbons versus number of cycles

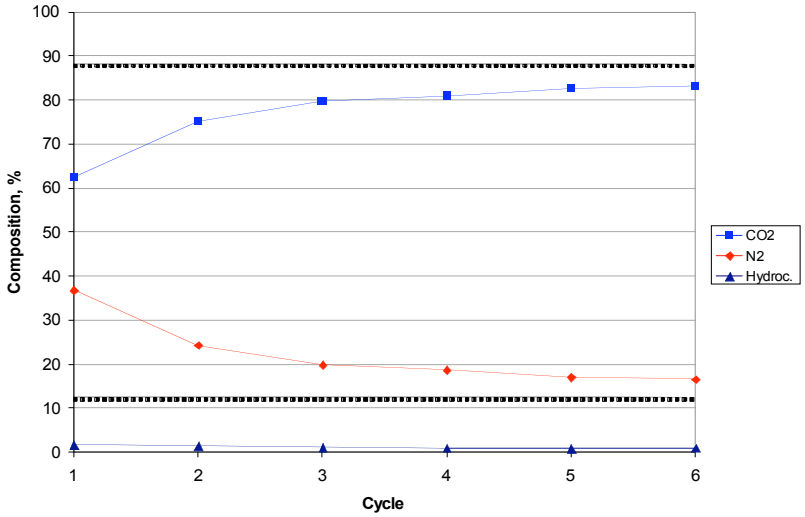

Figure 11: Experiment 2 gas composition, non-hydrocarbon components and total hydrocarbons versus number of cycles

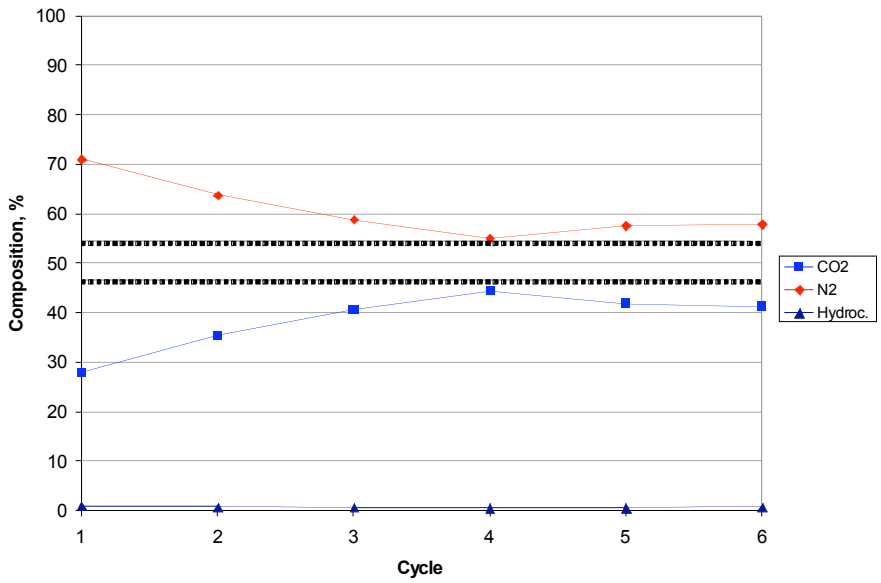

Figure 12: Experiment 3 gas composition, non-hydrocarbon components and total hydrocarbons versus number of cycles

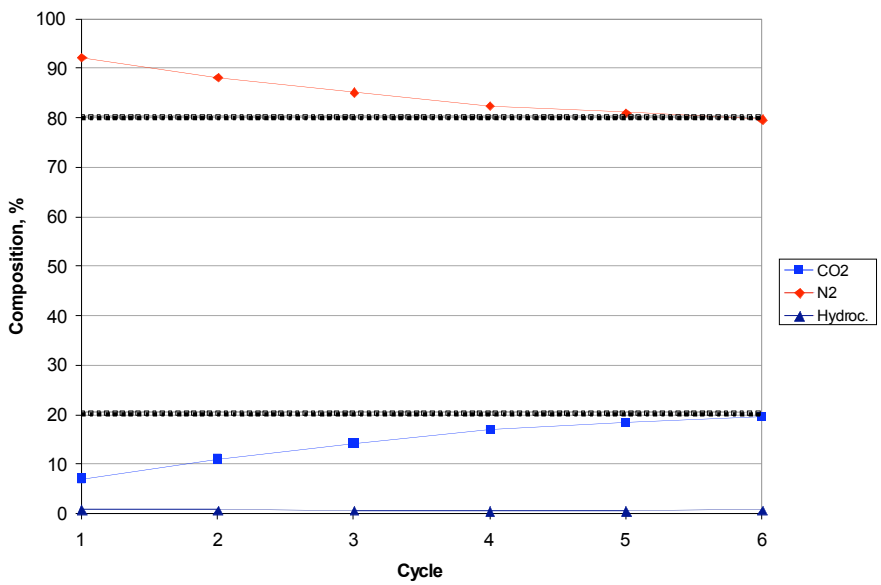

Figure 13: Experiment 4 gas composition, non-hydrocarbon components and total hydrocarbons versus number of cycles

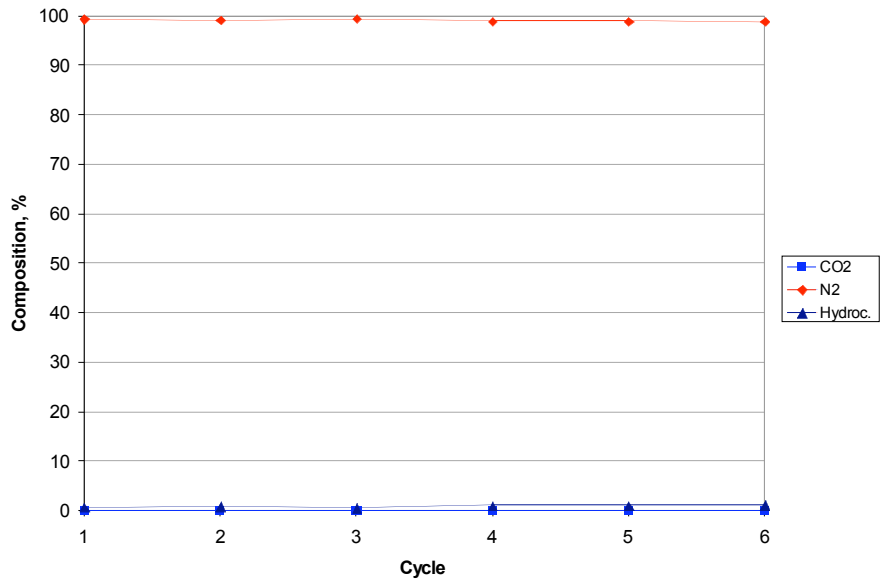

Figure 14: Experiment 5 gas composition, non-hydrocarbon components and total hydrocarbons versus number of cycles

Figures 10 to 14 illustrate the fact that injected gas (CO_2-N_2), under experimental conditions, goes into solution during the early cycles of the experiment. This is illustrated by the fact that the composition of the recovered gas is different from the gas injected. If the injected gas does not interact with the oil, the composition of the gas drawn from the PVT cell would be the same as the injected gas. Further, it was noted that with increasing cycles, the composition of the gas recovered from the PVT cell was similar to the gas injected. This illustrates that the solubility of the gas becomes less with an increase in cycles.

During the first three cycles, changes in the CO_2 and N_2 concentration contained in the recovered gas are more sensitive to the composition of the injected gas. For experiments with a low concentration of CO_2 (experiment 4), during the first four cycles the CO_2 percentage in the recovered gas varies from 7-% to 16-%. By contrast, the concentration of N_2 in the recovered gas decreased from 92-% to 82-%. In experiments with higher CO_2-concentrations in the injected gas (CO_2 concentration greater than 45-%), changes in non-hydrocarbon concentrations in the recovered gas are more appreciable. Experiments 1, 2, and 3 demonstrate an increase in CO_2 concentration of up to 20-% in the recovered gas. By contrast, N_2 exhibits a decrease in the concentration in the recovered gas of up to 19-%. During the last 2 cycles, variations in the amount of Carbon Dioxide and Nitrogen in the recovered gas were minimal. Changes amounted to only 1-%.

Figures15 to 19 contain plots of the change in the hydrocarbon composition in the recovered gas as a function of injection cycles. These charts reflect the sensitivity of each

of the oil components to vaporization. As the concentration of Carbon Dioxide increases in the injected gas, the hydrocarbon concentration in the recovered gas also increases.

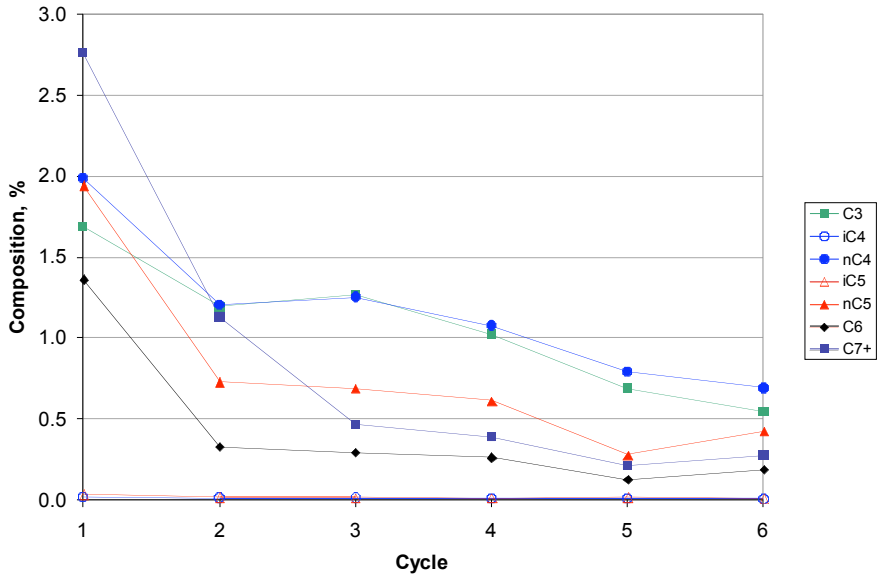

Figure 15: Experiment 1 gas composition versus cycle, hydrocarbon components

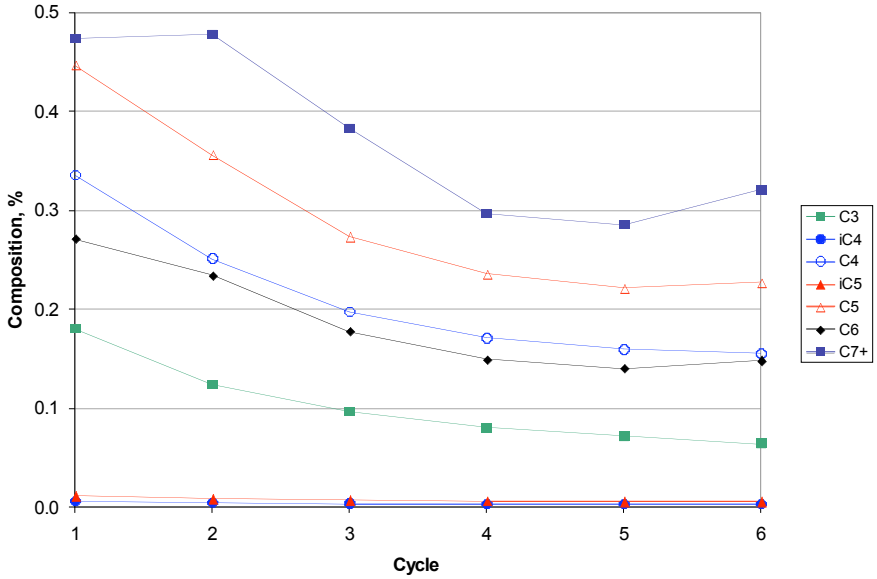

Figure 16: Experiment 2, gas composition versus cycle, hydrocarbon components

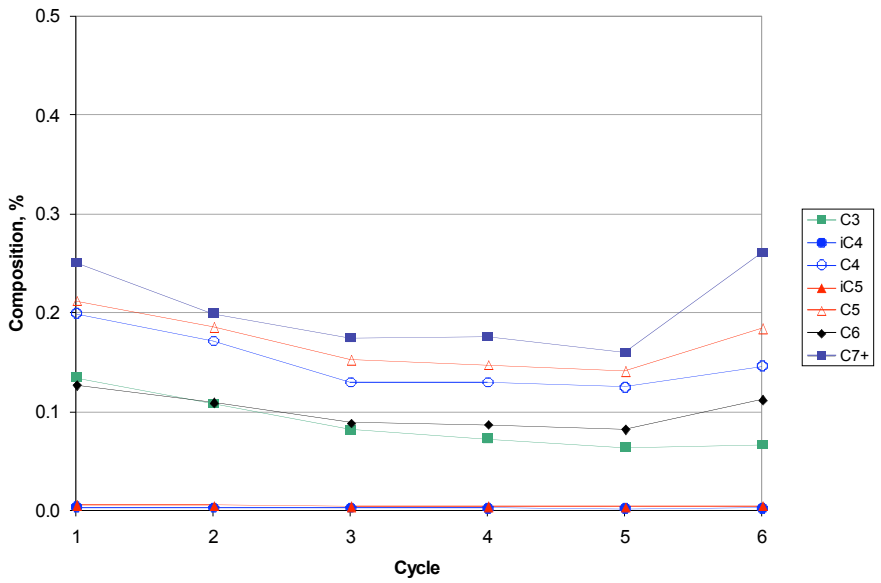

Figure 17: Experiment 3, gas composition versus cycle, hydrocarbon components

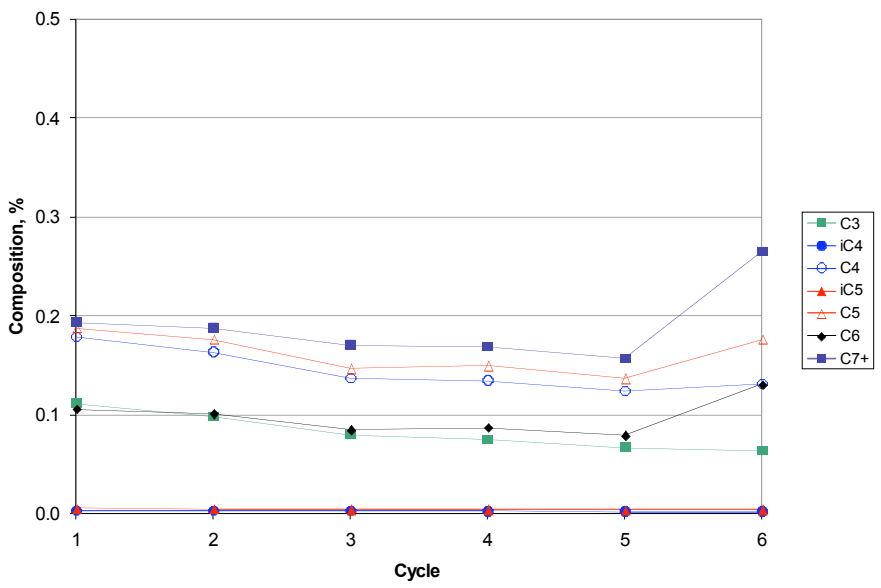

Figure 18: Experiment 4, gas composition versus cycle, hydrocarbon components

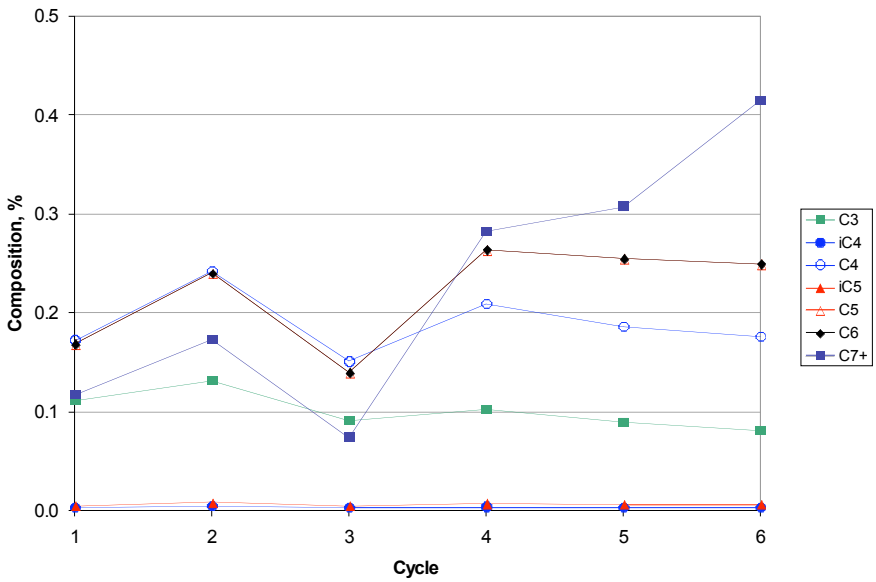

Figure 19: Experiment 5, gas composition versus cycle, hydrocarbon components

The hydrocarbon with the highest concentration in the recovered gas is C_{7+}, as shown in Table 3. This effect is because C_{7+} has the highest molar fraction in the original crude oil composition (0.88 molar-fraction). In addition, when CO_2 interacts with crude oil, it tends to vaporize the heavier hydrocarbon components from the crude oil (see Figures 15 to 19). By contrast, gases such as N_2 predominantly extract light and medium hydrocarbons, namely C_2 to C_5 (see Figure 18 and Figure 19).

The variation in composition versus the number of cycles illustrates the impact of number of cycles on the recovery process. Changes in the hydrocarbon composition of the recovered gas are more pronounced during the first four cycles of the experiment. This behavior is independent of the composition of the injected gas. For experiments using a high volume fraction of CO_2 (experiments 1 to 3), at the 4th cycle, the quantity of hydrocarbons in the recovered gas decreased by 50-% as compared to that in the first cycle. Figure 15 to Figure 19 show that the smaller the CO_2 content in the injected gas, the lower the hydrocarbon recovery. This is demonstrated by inspecting the plots on these figures and noting the differences in their slopes. During the transition from cycle 4 to cycle 5, the change in hydrocarbon composition is small and independent of Carbon Dioxide concentration.

To this point, we have discussed the effects of the injected gas on the compositions oil by studying the results of the gas analysis. The impact of these injected gases on crude oil is better seen using a pressure-temperature or phase-behavior diagram. Figure 20 and Figure 21 present phase behavior diagrams of the remaining crude oil in the PVT cell after six cycles of injection.

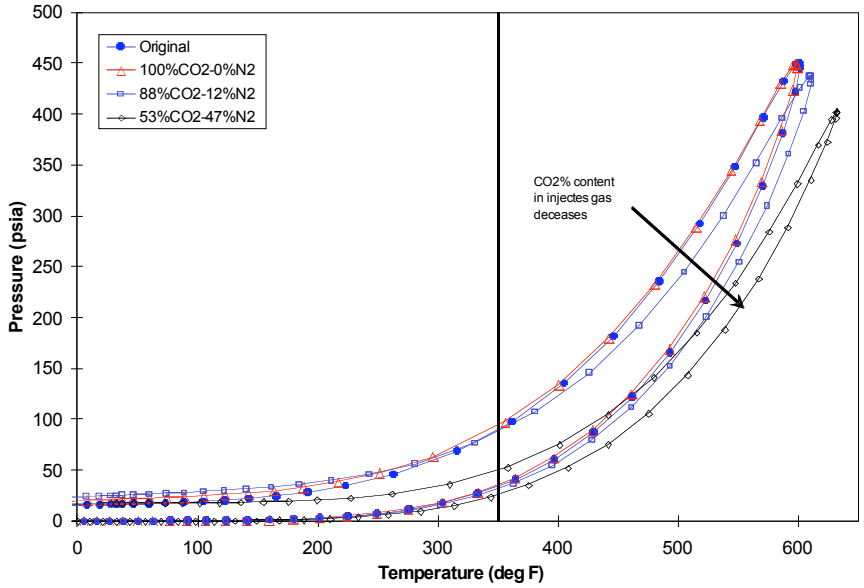

Figure 20: Sample 2 crude oil P-T diagram for experiments 1, 2 and 3 after 6 cycles

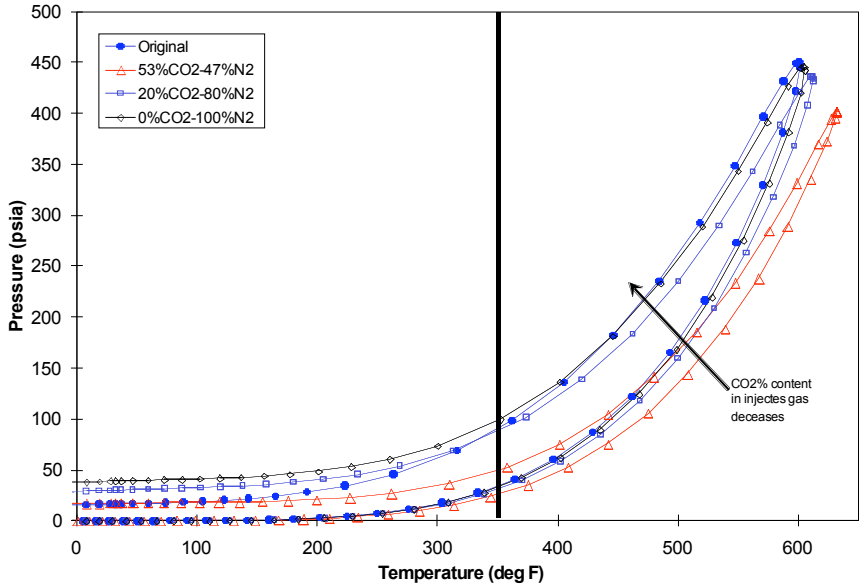

Figure 21: Sample 2 crude oil P-T diagram for experiments 3, 4 and 5 after 6 cycles

A focal point of this study is the changes in the composition of the crude oil that result from cyclic gas injection. In order to accomplish this objective, the composition of the crude oil remaining in the PVT cell at the conclusion of the experiment was determined. Figure 20 illustrates the changes in the oil phase diagram as the content of Carbon Dioxide in the injected gas is varied from 100-% to 53-% (experiments 1, 2 and 3). For conditions of pressure exceeding 200-*psia* and temperatures above 300-*ºF*, the effect of the gases used during cyclic injection is to shift the oil phase envelope to the right. For these mixtures, the lower the CO_2 concentration, the more pronounced the change in their respective phase envelopes. Figure 21 illustrates the P-T phase diagrams for crude oil as the concentration of CO_2 in the injection gas decreases from 53-% to 0-% (experiments 3, 4 and 5). For these experiments, decreasing the percentage of CO_2 in the injected gas results in a phase envelope of the final oil, that approximates the phase envelope of the original oil. For all the experiments where temperatures are lower than 350-º*F*, the dew point line remains unchanged whereas the bubble point pressure increases.

There are two reasons for the behavior of the phase envelope that were previously discussed. First, the changes in the phase diagrams are due to the fact that the composition of the oil changes as hydrocarbons are vaporized (primarily C_3-C_6) and CO_2 and N_2 are dissolved in the oil. Moreover, the vaporization of C_3-C_6 together with the characteristics of the injected fluid results in a relative increase in the mole-fraction of the heavy fraction, C_{7+}. Second, the composition of the injected fluid dictates the degree of shifting of the phase envelope. When pure components are injected (CO_2 or N_2), the phase envelope of the final oil is very similar to the phase envelope of the original composition. When mixtures of CO_2 and N_2 are used as injection fluid, the phase envelope shift is more pronounced. This is because CO_2 has the highest vaporization effect and replaces some of the extracted hydrocarbons in the crude oil. In the case of pure N_2, the main cause is its low molecular weight and its solubility in the oil.

Numerical results

Figure 22 illustrates a schematic of the laboratory experiments and illustrates the cyclic injection process. These data collected from these experiments were used as the underpinnings for the development of a phase behavior model (PBM). The PBM can then be used for fluid property predictions that are necessary for vapor-liquid equilibrium calculations in a reservoir simulator.

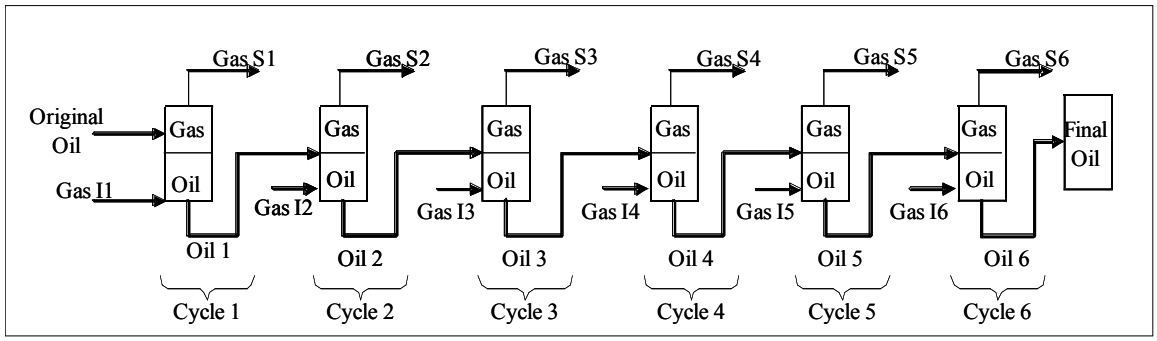

Figure 22: Schematic of experimental cyclic injection

The PBM is used at every cycle to perform the flash calculations and determine the equilibrium characteristics for the established pressure, temperature and overall mixture composition. Figure 23 to figure 34 show the match between compositions obtained from laboratory experiments and compositions predicted by the PBM.

In all the experiments, the gas composition after each cycle is primarily composed of non-hydrocarbon components (CO_2 and N_2). Figures 23 to 26 show the predictions of CO_2 and N_2 using the PBM as compared to that measured in the laboratory. The principal constituents in the gas phase are the injected gases (CO_2 and N_2). Only a small amount of these gases go into solution. Figures 27 to 30 show the portion of the injected gases predicted by the PBM that goes into solution. In the liquid phase, heavy components (C_7 to C_{10+}) represent 80-% to 95-% of the oil composition. Figures 31 to 34 show the values of C_7 to C_{10+} that were predicted using the PBM.

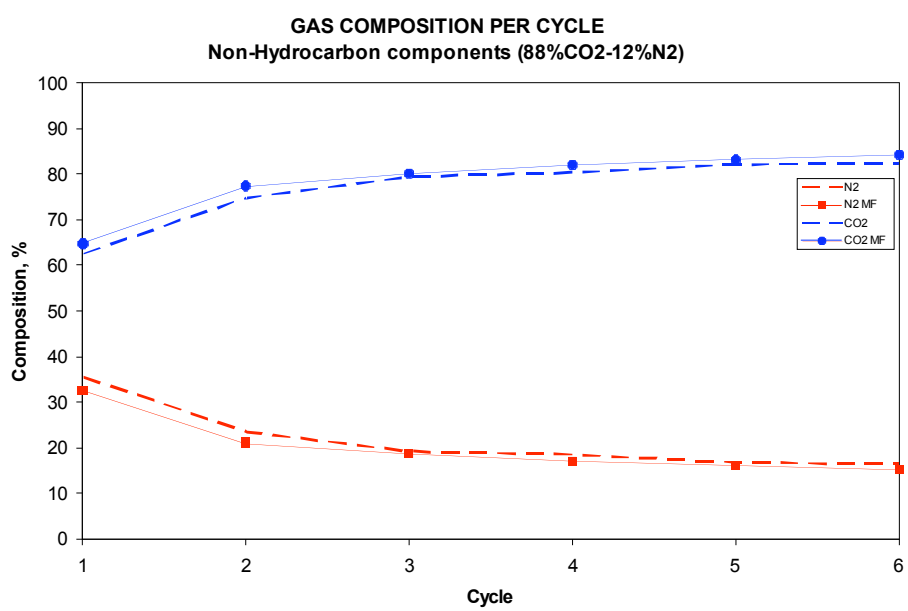

Figure 23: Gas composition from experiment 4 versus cycle, (non-hydrocarbons)

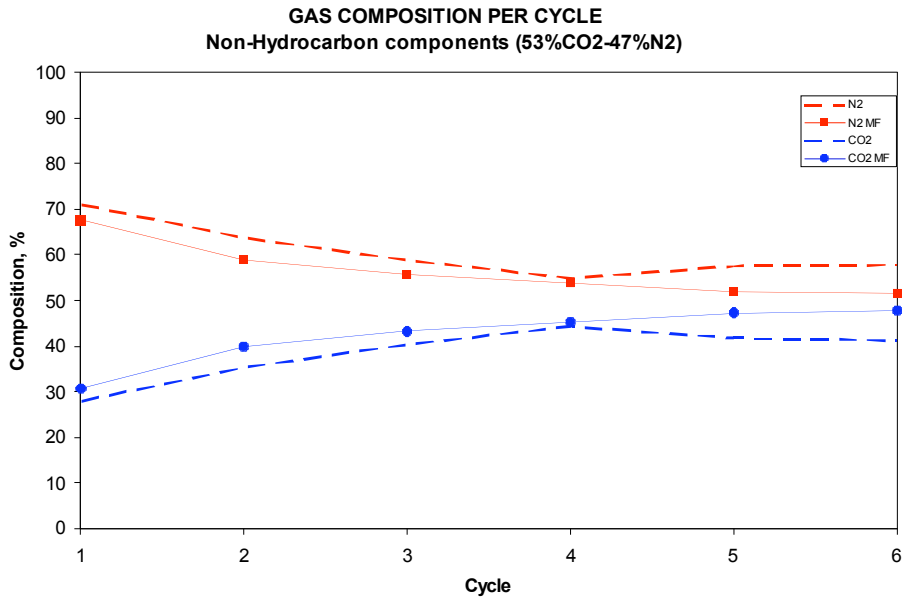

Figure 24: Gas composition from experiment 3 versus cycle, (non-hydrocarbons)

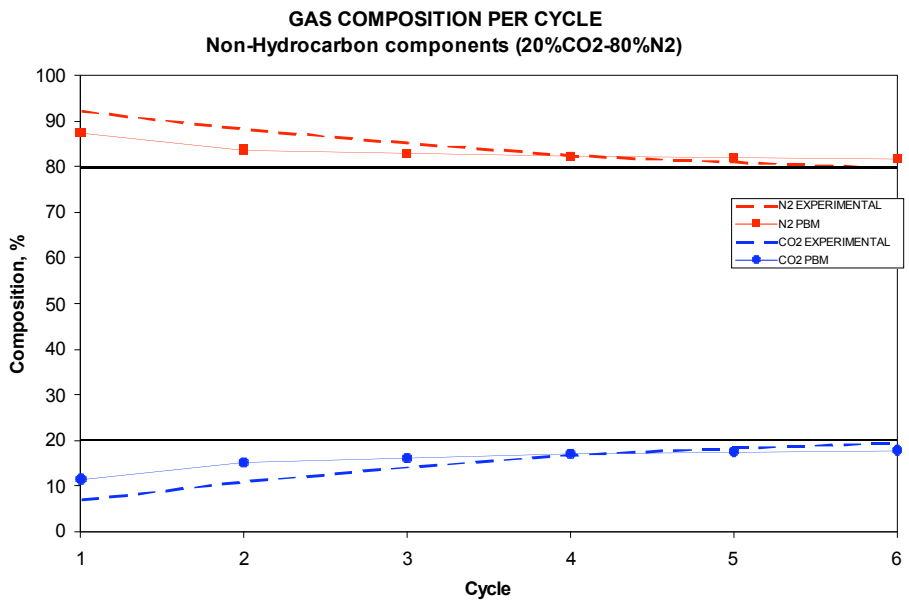

Figure 25: Gas composition from experiment 2 versus cycle, (non-hydrocarbons)

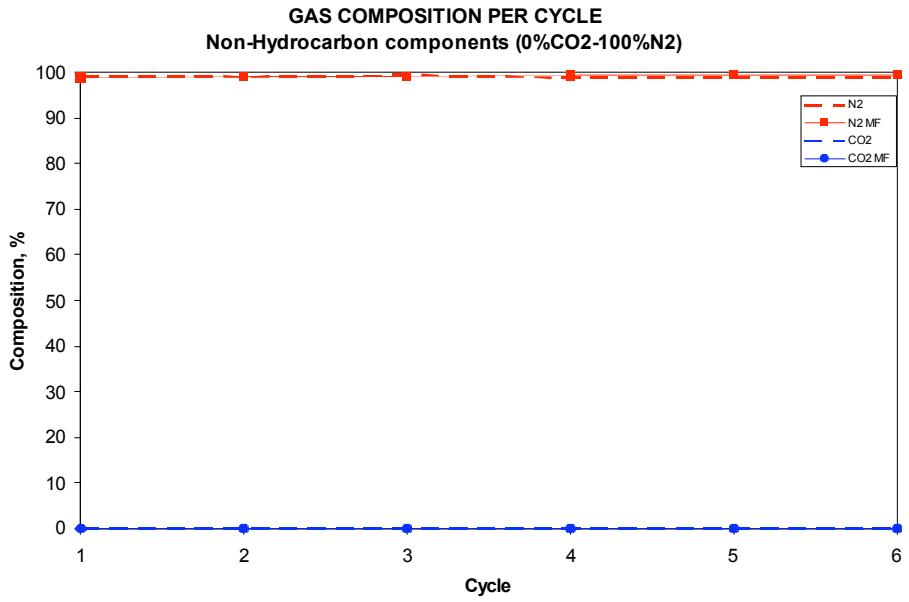

Figure 26: Gas composition from experiment 1 versus cycle, (non-hydrocarbons)

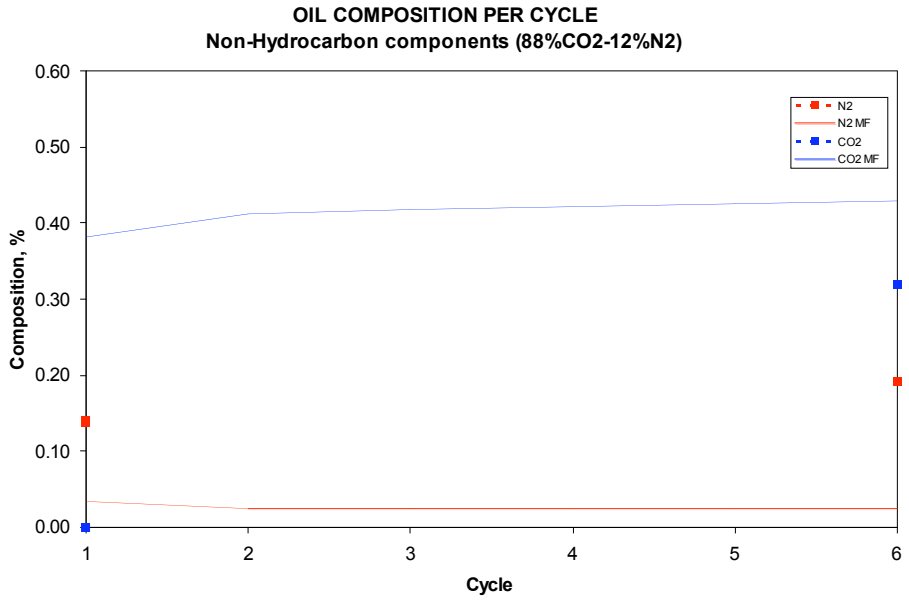

Figure 27: Oil composition from experiment 4 versus cycle, (non-hydrocarbons)

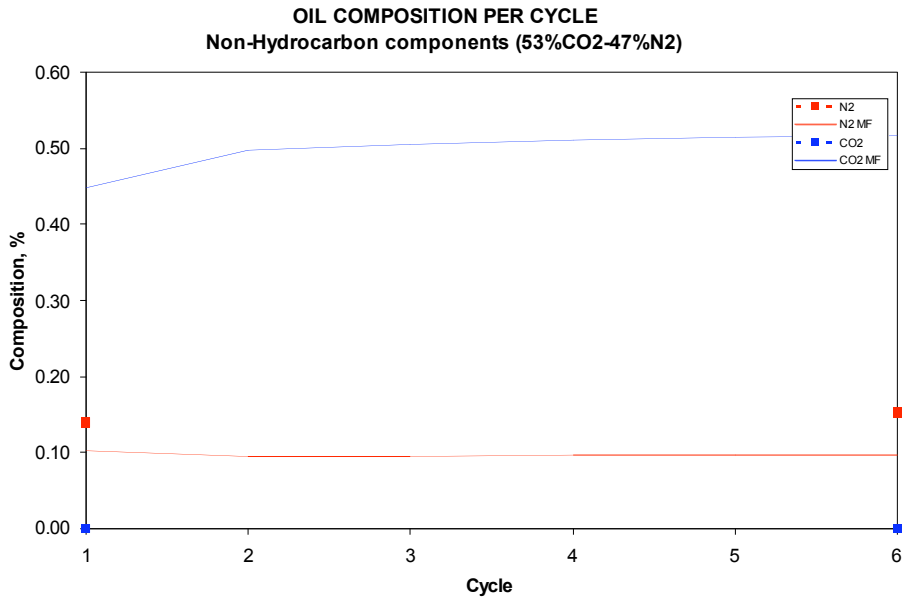

Figure 28: Oil composition from experiment 3 versus cycle, (non-hydrocarbons)

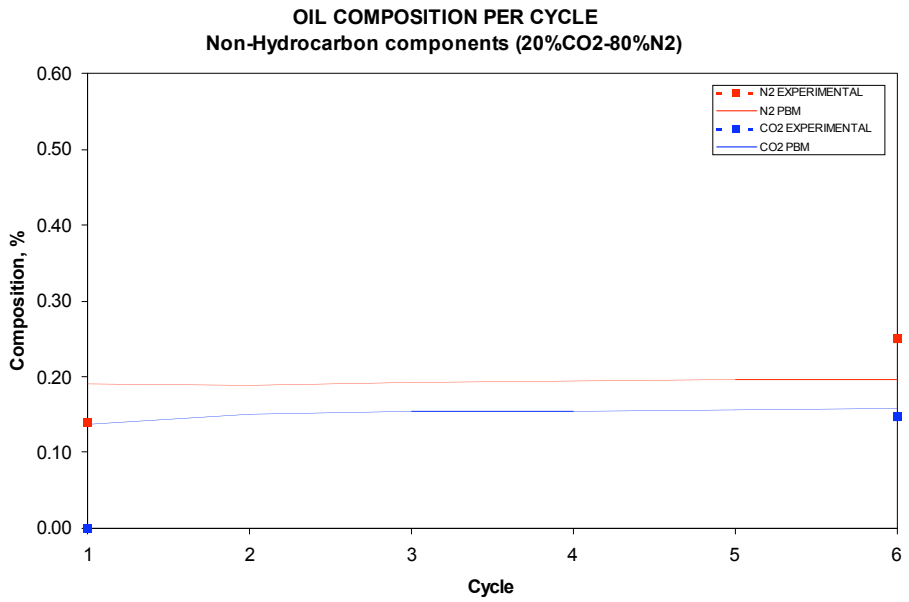

Figure 29: Oil composition from experiment 2 versus cycle, (non-hydrocarbons)

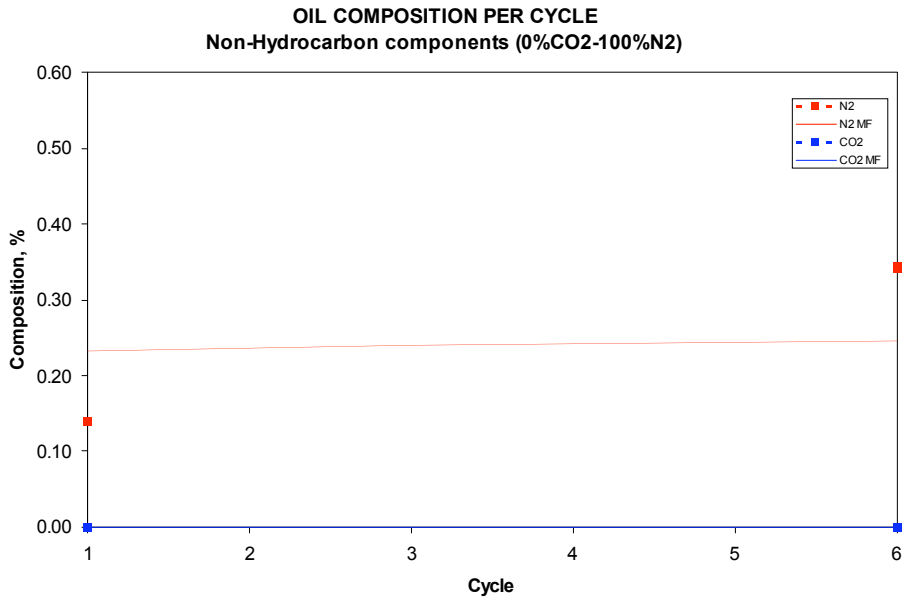

Figure 30: Oil composition from experiment 1 versus cycle, (non-hydrocarbons)

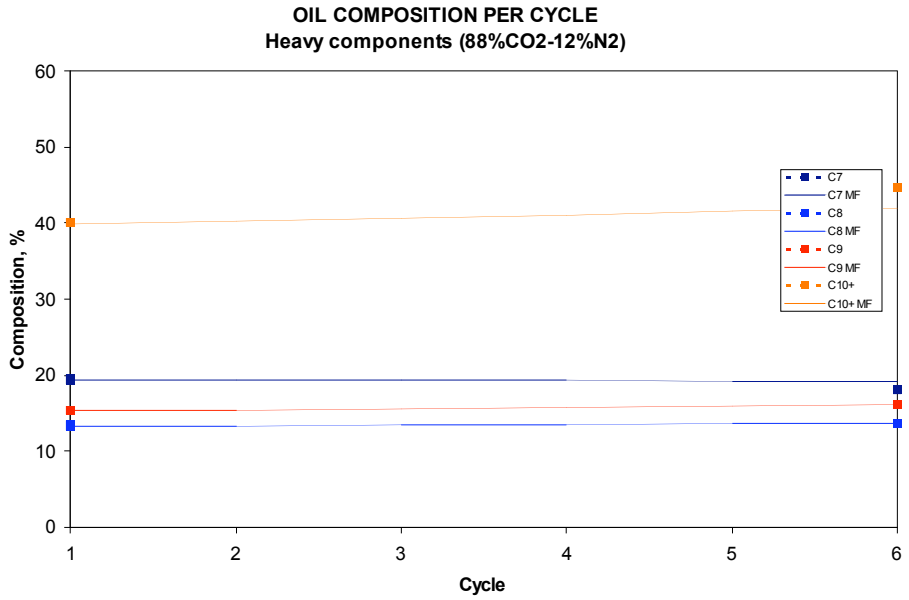

Figure 31: Oil composition from experiment 4 versus cycle, (C_7, C_8, C_9, C_{10+})

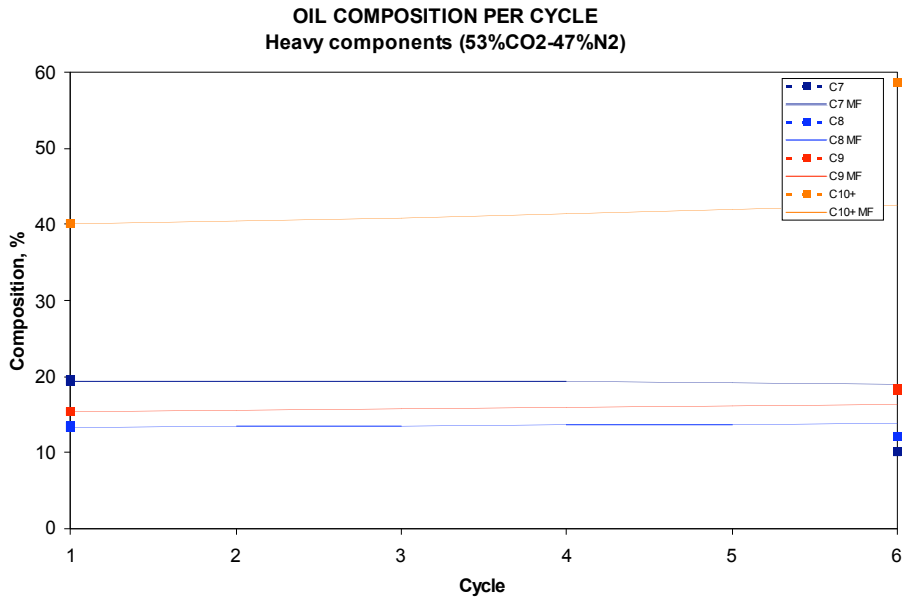

Figure 32: Oil composition from experiment 3 versus cycle, (C_7, C_8, C_9, C_{10+})

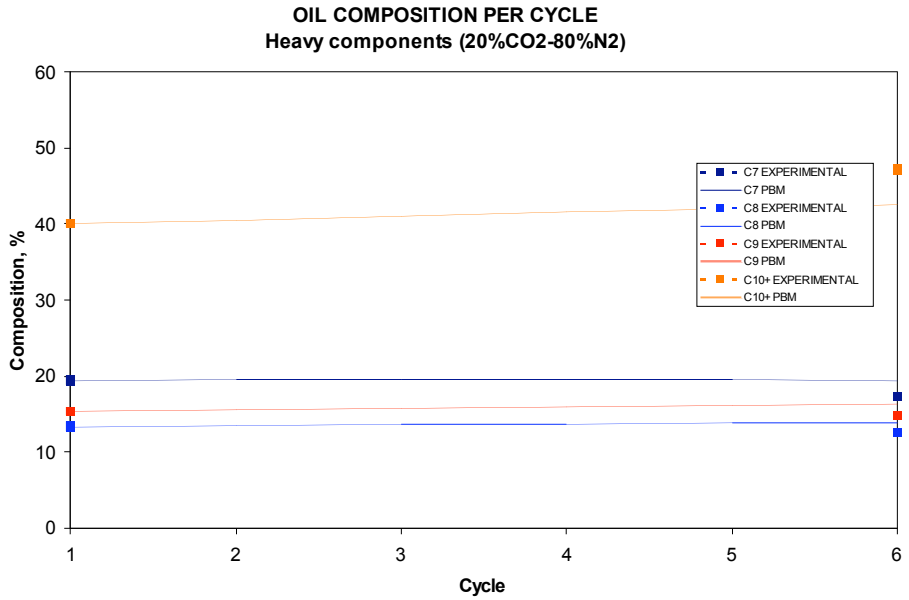

Figure 33: Oil composition from experiment 2 versus cycle, (C_7, C_8, C_9, C_{10+})

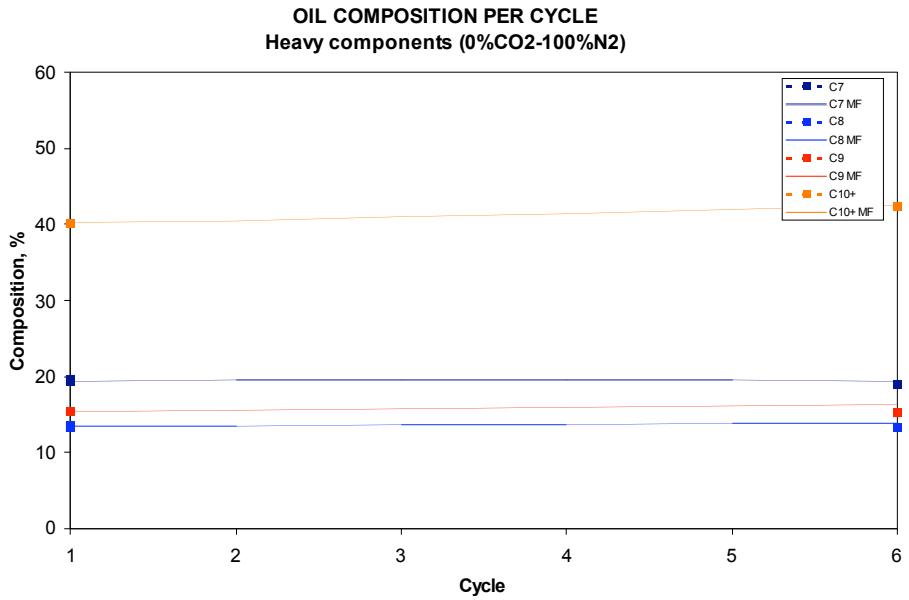

Figure 34: Oil composition from experiment 1 versus cycle, (C_7, C_8, C_9, C_{10+})

In summary, the PBM adequately predicts the compositions obtained from experiments. From previous investigations, Coats, K.H. and Smart, G.T. (1986) and Whitson, C. and Brule, M (2000), the improvement in PBM prediction capabilities was achieved by the modification of the EOS parameters. The modified parameters are: (i) the attraction parameter (Ω_a), (ii) the co-volume parameter (Ω_b), and (iii) the binary interaction coefficients (δ_{ij}). These modifications were not intended to be applied to all the mixture components, rather, specifically to methane, plus fractions, and non-hydrocarbon components.

CONCLUSIONS

Through laboratory experiments, a zero-dimensional model (PVT cell) was used to mimic the cyclic injection process and to develop an understanding of the behavior of crude oil when CO_2-N_2 gas mixture is injected into it. After finalization of the experimental part, we have a better understanding of the compositional changes occurring during the recovery process. Furthermore, a phase equilibrium model was developed to represent the thermodynamics of the cyclic injection process. The phase equilibrium package was used to replicate data generated during the experimental stage.

Moreover, the extrapolation of laboratory results to the field is not direct, but reasonable qualitative conclusions about the process can be drawn. Laboratory results indicate that CO_2 vaporizes more of the hydrocarbons in larger quantities than N_2, as shown in Table 3. Laboratory results also indicate that N_2 is more soluble than CO_2, 0.34-% mole-percent of N_2 compared to 0.17-% mole-percent of CO_2 when pure components are used as injected fluids. Finally, laboratory results show that CO_2 shows higher hydrocarbon vaporization effect than N_2 with maximum hydrocarbon extraction attained in concentrations close to 100-% in the injected fluid.

The tuned EOS adequately predicts the behavior of hydrocarbon components through cycles of injection-withdrawal. The tuning of EOS parameters, such as attraction parameter, the co-volume parameter, and the binary interaction coefficients, are of importance when matching experimental data. The tuning of these parameters is to be in the range of 5-% to 20-% of the values found in pertinent literature.

Future research

In spite of the fact that previous investigations have studied the cyclic injection technique, there remain uncertainties about the driving mechanisms attendant to this process as well as the strategy that would maximize recovery. There are a number of variables involved in the design of a successful and profitable gas cyclic operation. The focus of forthcoming studies will be to investigate the influence of these variables on the cyclic injection process and to determine their optimum values during cyclic operations

Furthermore, the phase equilibrium model developed represents the thermodynamics of the cyclic injection process. This phase equilibrium package will be used for fluid properties determination and in vapor-liquid equilibrium calculations embedded within a compositional reservoir simulator. The reservoir model will be able to handle compositional changes occurring in the reservoir. Among the characteristics of its configuration are: single well reservoir (radial-cylindrical coordinates), three-dimensional systems (r-z), three-phase system (oleic, gaseous and aqueous phases).

A parametric study will be used to test the sensitivity of critical design parameters in cyclic injection process. Such parameters are slug size of injected fluid, soaking time,

number of cycles, injection conditions of pressure and rate, injection fluid quality, and reservoir pressure, among others. The parametric study will allow us to develop insights concerning the driving mechanisms attendant to the cyclic injection process.

Since the goal is to optimize the gas cyclic injection process, attention must be given to how and when the reservoir should be restimulated. Either continue production or shut-in the well and restimulate, the decision must be made. If the decision is to restimulate, one must decide about the amount of gas to be injected, rate of injection, pressure of injection, and so forth. All of these decisions should be made considering the entire process, rather than each particular stage. This is because every action will affect the process over the remainder of its life. The primary goal at this stage will be to develop a dynamic programming model to optimize the gas cyclic injection problem.

A previous investigation that used dynamic programming as optimization tool was Bentsen, R.G and Donohue, D. A. (1969). Bentsen and Donohue applied the dynamic programming model to optimize the cyclic steam injection process. In their work, the problem was to select the optimum number and size of steam treatments to maximize the profits over the entire life of the project. They found that by applying an optimal policy, a more efficient use of steam and time was realized, and profits were increased by 23%. A similar optimization scheme is under development and will be used in this investigation.

REFERENCES

Al-Wadhahi, M., Boukadi, F.H., Al-Bemani, A., Al-Maamari, R. and Al-Hadrami, H., 2007. Huff 'n puff to revaporize liquid dropout in an Omani gas field. Journal of Petroleum Science and Engineering 55(1-2): 67-73.

Ayala, L.F., 2004. Compositional modeling of naturally-fractured gas-condensate reservoirs in multi-mechanistic flow domains. Thesis (Ph.D.) Thesis, Pennsylvania State University, 2004., 212 leaves pp.

Aziz, K. and Settari, A., 1979. Petroleum Reservoir Simulation. . Applied Science Publishers, London, xxi, 476 p. pp.

Brock, W.R. and Bryant, L.A., 1989. A summary result of CO_2 EOR field tests, 1982 - 1987. SPE Paper 18977 presented at the 1989 Reservoir Symposium(6-8 March).

Denoyelle, L.C., Lemonniere, P., 1987. Simulation of CO_2 Huff'n Puff using relative permeability hysteresis. SPE Paper 16710 presented at the 1987 ATCE(27-30 September).

Emanuel, A.S., Tang, R.W., Fong, W.S. and Langston, M.V., 1991. Analytical and numerical model studies of cyclic CO_2 injection projects. SPE Paper 22934 presented at the 1991 ATCE(6-9 October).

Ertekin, T., Abou-Kassem, J. H., King, G. R., 2001. Basic applied reservoir simulation. SPE textbook series ; v. 7 SPE Paper. Society of Petroleum Engineers, Richardson, Tex., xii, 406 p. pp.

Haskin, H.K. and Alston, R.B., 1989. An evaluation of CO_2 Huff'n Puff test in Texas. Journal of Petroleum Technology (February).

Hsu, H.H. and Brugman, R.J., 1986. CO2 Huff'n Puff using a compositional reservoir simulator. SPE Paper 15503 presented at the 1986 ATCE(5-8 October).

Jarrell, P.M., Fox, C. M., Stein, M. H., Webb, S. L., 2002. Practical aspects of CO_2 flooding. SPE monograph series SPE Paper, 22. Society of Petroleum Engineers, Richardson, Texas, vii, 220 p. pp.

Miller, B.J. and Bardon, C.P., 1994. CO_2 Huff'n Puff field case: Fiver year program update. SPE Paper 27677 presented at the 1994 Permian basin oil and gas recovery (16-18 March).

Mohammed-Singh, L., Singhal, A.K. and Sim, S., 2006. Screening criteria for Carbon Dioxide Huff'n Puff operations. SPE Paper 100044 presented at the 2006 Symposium on improved oil recovery(22-26 April).

Monger, T.G. and Coma, J.M., 1988. A laboratory and field evaluation of CO_2 Huff'n Puff process for light oil recovery. SPE Paper 15501 presented at the 1988 ATCE(5-8 October).

Patton, J.T., Coats, K.H. and Spence, K., 1982. Carbon Dioxide well stimulation: Part 1 - A parametric study. Journal of Petroleum Technology, SPE Paper 9228(August): 1798-1804.

Simpson, M.R., 1988. The CO_2 Huff'n Puff process in a Bottom water drive reservoir. Journal of Petroleum Technology(September): 887.

Thomas, J., Berzins, T.V., G., M.T. and Bassiouni, Z., 1990. Light oil recovery from cyclic CO_2: Influence of gravity segregation and remaining oil. SPE Paper 20531 presented at the 1990 ATCE(23-26 September).

Whitson, C.H., Brulâe, M.l R., 2000. Phase behavior. Henry L. Doherty Memorial Fund of AIME, Society of Petroleum Engineers, Richardson, Tex., vi, 233 p. pp.

NOMENCLATURE

Romans

A = Peng-Robinson attraction parameter, dimensionless
B = Peng-Robinson co-volume parameter, dimensionless
b_i = component co-volume parameter, dimensionless
b_m = mixture co-volume parameter, ft^3 / lbmoles
c_i, c_j = mole fraction of component in the phase, dimensionless
f_{li} = fugacity of component '*i*' in the liquid phase, psia
f_{gi} = fugacity of component '*i*' in the gas phase, psia
f_{ng} = vapor fraction in the mixture,
K_i = equilibrium constant ratio for component i, dimensionless
Mw = Molecular weight, lb/lbmol
p = system pressure, psia
p_{ri} = component reduced pressure, dimensionless
R = universal gas constant, 10.73 psia ft^3 / lbmoles ºR
T_{ri} = component reduced temperature, dimensionless
T = system temperature, ºR
v_m = molar volume, ft^3 / lbmoles
x_i = molar fraction of component 'i' in the liquid phase, dimensionless
y_i = molar fraction of component 'i' in the vapor phase, dimensionless

Greeks

$(a\alpha)_m$ = mixture attraction parameter, psia $(ft^3)^2$ / $lbmoles^2$
$(a\alpha)_i$ = component attraction parameter, dimensionless
δ_{ij} = binary interaction coefficient between component 'i' and component 'j', dimensionless
ϕ_i = fugacity coefficient of component '*i*', dimensionless
μ_g = viscosity of aqueous phase, lb/ft^3
μ_l = viscosity of liquid phase, lb/ft^3
Ω_{ai} = component attraction parameter constant, dimensionless
Ω_{bi} = component co-volume parameter constant, dimensionless
ρ_g = density of gas phase, lb/ft^3
ρ_l = density of liquid phase, lb/ft^3
ω_i = component Pitzer's accentric factor, dimensionless

Subscripts

i	= component
j	= component
m	= overall mixture
g	= gas phase
l	= liquid phase
f	= flowing phase, g=gas, l=liquid